POLITECNICO
DI TORINO

CHALMERS
UNIVERSITY OF TECHNOLOGY

Assessment of AEB algorithms and relevance of datasets used for AEB assessment

Master's thesis in Automotive Engineering

PIERLUIGI OLLEJA

POLITECNICO DI TORINO - ITA
CHALMERS UNIVERSITY OF TECHNOLOGY – SWE

MASTER'S THESIS IN AUTOMOTIVE ENGINEERING

Assessment of AEB algorithms and relevance of datasets used for AEB assessment

PIERLUIGI OLLEJA

Department of Mechanics and Maritime Sciences
Division of Vehicle Safety
Unit of Crash Analysis and Prevention
CHALMERS UNIVERSITY OF TECHNOLOGY - SWE

DIMEAS - Dipartimento di Ingegneria Meccanica e Aerospaziale
POLITECNICO DI TORINO - ITA

Assessment of AEB algorithms and relevance of datasets used for AEB assessment
PIERLUIGI OLLEJA

Master's Thesis 2019:83
Department of Mechanics and Maritime Sciences
Division of Vehicle Safety
Unit of Crash Analysis and Prevention
Chalmers University of Technology - SWE
DIMEAS - Dipartimento di Ingegneria Meccanica e Aerospaziale
Politecnico di Torino - ITA

Telephone: + 46 (0)31-772 1000

Cover:
Logo of Politecnico di Torino and Chalmers University of Technology.

Chalmers Reproservice / Department of Mechanics and Maritime Sciences
Göteborg, Sweden 2019-09-11

Assessment of AEB algorithms and relevance of datasets used for AEB assessment
Master's thesis in Automotive Engineering
PIERLUIGI OLLEJA
Department of Mechanics and Maritime Sciences
Division of Vehicle Safety
Unit of Crash Analysis and Prevention
Chalmers University of Technology
DIMEAS - Dipartimento di Ingegneria Meccanica e Aerospaziale
Politecnico di Torino

Abstract

Road fatalities are a major concern in modern society. The increase in the amount of road vehicles on public roads exposes more people to the dangers that come with road traffic. On highways, higher speeds are the cause of more serious crashes. To tackle this issue, active safety systems work in cooperation with passive safety systems to improve the occupants' safety. In the assessment of new active safety systems, the availability of crashes for computer simulation is limited. This work is therefore aimed first at using lead-vehicle-braking events from the highD naturalistic driving dataset as a basis for creating "what-if" crashes. These crashes were compared with real crashes from an in-depth crash database (GIDAS) and an AEB algorithm was assessed on both the datasets. The assessment was done using a common simulation framework, developed in this work, and the results of crash avoidance and mitigation were compared. Both datasets were collected on German highways. The results showed comparable trends for the relative velocities involved in crashes from both datasets, when comparing crashes where there was no reaction by the driver of the following vehicle. The AEB assessment didn't show clear similarities in crash avoidance and mitigation.

Key words: Automated Emergency Braking (AEB), naturalistic driving dataset, counterfactual simulations, rear-end collision, crash avoidance.

Contents

Abstract I
Contents III
Preface V
Acknowledgements V
Notations VI
1 Introduction 1
2 Method 5
2.1 highD data processing 5
2.1.1 Master clock synchronization 5
2.1.2 Assessment of critical scenarios 6
2.1.3 Crash generation 7
2.2 PCM metrics extrapolation 9
2.2.1 Range 10
2.2.2 Lateral offset 13
2.3 AEB implementation 13
2.3.1 Vehicle limits 14
2.3.2 Algorithm 14
2.3.3 Modification of the scenario 16
2.4 Analysis methods 19
3 Results 20
3.1 GIDAS-PCM and highD crash comparison 20
3.2 AEB implementation on PCM 21
3.3 Comparison between AEB in PCM and highD crashes 23
4 Discussion 28
4.1 Discussion of results 28
4.2 Limitations 30
4.2.1 Methods 30
4.2.2 Data 32
4.3 Future work 32
5 Conclusion 34
6 References 35

Preface

This study is a master thesis work carried out at Autoliv Development (industry) and at the Department of Mechanics and Maritime Sciences, Division of Vehicle Safety, Unit of Crash Analysis and Prevention, Chalmers University of Technology, Sweden (academic institution). The work was performed during the ERASMUS+ study exchange program, for the home university Politecnico di Torino, MSc in Automotive Engineering. The work was developed from January to August 2019 in the Vehicle and Traffic Safety Centre at Chalmers - SAFER, in Göteborg, and occasionally in Autoliv, in Vårgårda.

Acknowledgements

First, I would like to express my gratitude to the examiner and supervisor of the project Jonas Bärgman and to the supervisor Nils Lubbe, for your constant willingness to help and to support me in any situation and for the trust you put in me. I was amazed by how easily and immediately I felt comfortable working with you. I would also like to thank everyone else working in SAFER, as thanks to you I felt immediately at ease in this new working environment. I thank also the supervisor from Italy Andrea Tonoli, from Politecnico di Torino. A special thanks goes to Xiaomi and Sabino, for all the hours of intense problem-solving sessions until late evening, that helped in the development of this work.

I am very grateful to my family, that constantly supported me in this experience far from home and that showed enthusiasm and trust in me in everything I was doing. Finally thanks to all my friends, the ones I met in Sweden from all over the world and the friends from Italy, that always supported me during difficult times.

Göteborg September 2019-09-11

PIERLUIGI OLLEJA

Notations

Abbreviations

AEB	Automated Emergency Braking
AES	Automated Emergency Steering
BTN	Brake Threat Number
COG	Centre Of Gravity
Delta-V	Delta Velocity
ERSO	European Road Safety Observatory
FCW	Forward Collision Warning
FV	Following Vehicle
GIDAS	German In-Depth Accident Study
LDW	Lane Departure Warning
LKA	Lane Keeping Assist
LV	Leading Vehicle
NDD	Naturalistic Driving Dataset
NGSIM	Next Generation Simulation
NHTSA	National Highway Traffic Safety Administration
OICA	Organisation Internationale des Constructeurs d'Automobiles (English: International Organization of Motor Vehicle Manufacturers)
PCM	Pre-Crash Matrix
PDF	Probability Density Function
P.E.A.R.S.	Prospective Effectiveness Assessment of Road Safety
SAE	Society of Automotive Engineers
SHRP2	Strategic Highway Research Program 2
STN	Steering Threat Number
THW	Time Headway
TTC	Time To Collision
WHO	World Health Organization

Symbols

a_{FV}	Acceleration of FV
a_j	Acceleration of FV including jerk
a_m	Needed constant acceleration to avoid the collision
a_{max}	Maximum deceleration reachable by the FV
$a_{max,lat}$	Maximum lateral acceleration reachable by the FV
$\widetilde{a_{max}}$	Maximum between a_{max} and $a_{FV}+j_{max}t_s$
a_{LV}	Acceleration of LV
a_{req}	Acceleration required to avoid the collision
$a_{req,lat}$	Lateral acceleration required to avoid the collision
c_{highD}	Slope for highD linear regression model
c_{PCM}	Slope for PCM linear regression model
d_{COG-f_a}	Distance between COG of the vehicle and front bumper
f_i	i-th frame
f_r	Frame rate
j_{max}	Maximum jerk reachable by the FV
l	Length of the vehicle
p_{RECT}	Matrix containing vehicle vertices coordinates

p_{ROT}	Matrix containing rotated vehicle vertices coordinates
p_{TRAS}	Matrix containing rotated and translated vehicle vertices coordinates
q_{highD}	Intercept for highD linear regression model
q_{PCM}	Intercept for PCM linear regression model
r	Range
$\dot{r}$	Range rate
$\ddot{r}$	Range acceleration
r_0	Initial range
$\dot{r}_0$	Initial range rate
R_{lat}	Lateral offset
t	Time
t_0	Initial time
t_d	Time delay of the braking system
t_i	i-th instant of time
t_s	Time required to stop the vehicle
v_0	Initial speed
v_{FV}	Speed of FV
v_{LV}	Speed of LV
w	Width of the vehicle
x_0	Initial position
x_{POS}	x position
y_{POS}	y position
ϑ	Angle between transversal planes of the vehicles
ρ	Radius of curvature from centreline of the path
ρ_v	Distance between vertices of vehicles and centre of the circumference
ψ	Yaw angle
$\dot{\psi}$	Yaw angle rate

1 Introduction

Transportation by means of road vehicles has seen an increase of the motorization rate (number of vehicles / 1000 inhabitants) from 2005 to 2015 of 27% worldwide, with the total number of vehicles on the road reaching over 1.2 billion units (OICA, 2018). Traffic crashes are the 8th most common cause of death worldwide and the first cause of death for young people aged between 5 and 29 (WHO, 2018). The number of killed world-wide in traffic in 2016 was estimated to 1.35 million people. In Europe in 2015 25,651 people died in a car crash, resulting in a decrease of road fatalities of -1.8% compared to the previous year (ERSO, 2018a). Within the fatal road crashes in 2016, 8% happened on the motorway showing a decrease of -2.2% of the fatalities compared to the previous year in this scenario (ERSO, 2018b).

Although the number of vehicles on the road is increasing worldwide, the number of deaths for every 100,000 vehicles decreased by more than 50% in the period from 2000 to 2016 (WHO, 2018). This result shows how occupant protection systems, law enforcement and rescue actions improved in the last decades. For occupant protection systems, passive safety systems are aimed at protecting the occupants from the consequences of a crash (ERSO, 2018c). Active safety systems are instead aimed at avoiding or mitigating road crashes by actively monitoring the surroundings of the vehicles, trying to reduce the situations in which passive safety systems would need to deploy (Hamid, 2007). Avoiding or mitigating crashes using active safety systems can be performed deriving metrics of the surroundings and by means of threat assessment algorithms performing actions on the systems on a vehicle. Active safety systems act on different level, differentiating in warning only systems and intervention systems (SAE, 2015). Warning-only active safety systems inform the driver about potential hazardous situations. Examples include Forward Collision Warning (FCW), warning the driver when a collision is imminent (but can be avoided by braking) and Lane Departure Warning (LDW) when a steering action is required to avoid road a departure. Intervention active safety systems involve the actuation of vehicle systems without necessarily requiring an action from the driver, e.g. Automated Emergency Braking (AEB), Automated Emergency Steering (AES) and Lane Keeping Assist (LKA), in which brake and steering inputs are automatically given to the vehicle to avoid imminent crashes, or, for LKA just steering to keep the vehicle in the current lane.

Rear-end collisions are among the most common types of crashes for which intervention strategies of collision avoidance or mitigation have been proposed. Brännström et al. (2008) proposed a collision avoidance system working both on the longitudinal control (braking) and the lateral control (steering) of the vehicle. In this paper, the Brake Threat Number (BTN) and the Steering Threat Number (STN) were values computed based on vehicles positions, speeds and accelerations, to set a threshold for the intervention of the vehicle systems. This is the threat-based approach, that uses the required deceleration/lateral offset needed to avoid the crash. The BTN (see Section 2.3.2) is computed as the ratio between the required acceleration to avoid the collision and the maximum deceleration that the vehicle can reach. The STN (see Section 2.3.2) is instead the ratio between required lateral acceleration to avoid the crash, function of the lateral offset and the Time to collision (TTC), and the maximum lateral acceleration reachable by the vehicle. The work was continued by proposing an improved version of the algorithm (Brännström et al., 2010), that included a study of the capacity of drivers performing evasive manoeuvre,

to decrease false interventions of the system. Collision avoidance by steering was also proposed by Eidehall et al. (2007) and by Hac, Dickinson (2006).

The assessment of effectiveness of safety systems can be obtained with computer simulation starting from real crash scenarios and applying to them the active safety system (Kusano and Gabler, 2012). The safety assessments of AEB algorithms in simulated environment does not require real vehicles and test tracks, so their use can be more convenient than a real experiment as more simulations can be run in different scenarios, especially at an early stage of the system development. A comprehensive review of the active safety system assessments methods was presented by the P.E.A.R.S. (Prospective Effectiveness Assessment for Road Safety) consortium (Alvarez et al., 2017). They proposed a summary of the research questions and of the relevant metrics used when assessing active safety systems. They also proposed a framework that started with a reference situation (i.e., without the safety system), followed by the application of the system. By comparing the relevant metrics obtained as outcomes from the system implementation, (e.g. the amount of crash avoided or the mitigation of the crashes and of the crash related injuries) between the reference and system simulations, the benefit of a system can be estimated. General research questions and relevant metrics for the assessment criteria, combined with more specific simulations of systems (Erbsmehl, 2009) form the basic concept for the development of a framework for the simulation-based assessment of active safety system. The results from these types of assessments can have different consequences at different levels. From metrics related to single crashes, such as crash avoidance or mitigation, the immediate benefits of a systems on the single crashes can be studied. More long-term analysis, related to the impact of systems on the society, can lead instead to analysis for long-term safety benefits, lives saved and economic impact. Types of assessments can also be divided in the retrospective and prospective approaches (Alvarez et al., 2017). The retrospective approach can be performed on a system that is already available on the market by analysing real data of vehicles on the road with and without the safety system. The prospective approach consists instead in making predictions about the future effectiveness of an under-development safety system using virtual simulations.
As it might be difficult to reach a market penetration that is meaningful for an analysis before a long time from the introduction of the system (Sander, 2018), (Sander, Lubbe, 2018a), a proactive approach could be preferred.

A method used in the virtual assessment of active safety system is what-if/counterfactual simulations. What-if/counterfactual simulations use a part of the real data available and modify selected conditions, allowing for example an inclusion of an active safety system. The performances and effects of an active safety system can be therefore evaluated in a simulated environment, using data from real crashes or near-crashes (Kusano and Gabler, 2012; McLaughlin et al., 2008; Bärgman et al., 2015). Virtual simulation environments allow for the use of different types of datasets. Real crash datasets and Naturalistic Driving Datasets (NDD) are two examples of datasets, each having their advantages and disadvantages (Sander, 2018; McLaughlin et al., 2008, Bärgman et al., 2015). The main difference between the two types of datasets is that real crash datasets only contain crashes really happened on the road, whereas NDDs contain scenes of everyday driving scenarios. For this reason NDD seldom include crashes, and they require an additional step that consists in the generation of crashes, before the actual safety system implementation can be performed (Bärgman et al., 2017; Woodrooffe et al., 2012). In this way it is potentially possible to obtain several new crashes to test from the more common near-

crash situations that are present in NDD. However, care must be taken with the generalizability of the results when using generated crashes, because validation should be performed (Bärgman et al., 2015). The application of driver models to counterfactual simulations has also to be taken into account to have better fidelity with respect to real crashes when active safety systems are assessed (Bärgman et al., 2017). Nevertheless such driver models are more useful when the driver is active during the functioning of an active safety system, that is not the case in an AEB implementation as the vehicle performs all the evasive manoeuvre excluding the driver completely.

The selection of the data used in the assessment of an active safety system is therefore of key importance. To be able to replicate crashes in a simulated environment, a detailed description of the kinematics of a crash is needed. Police reported crashes are often not sufficiently accurate and consistent in the classification of the crash severity and the crash contributing factors are not sufficiently detailed (Otte et al., 2003; Imprialou, Quddus, 2017). Moreover, crashes without severe injuries are underreported (Abay, 2015; Imprialou, Quddus, 2017). In the year 2000 21% of the injuries occurred in crashes that were not reported by the police (Blincoe et al., 2002). A more detailed description of crashes can be found in the so-called in-depth crash databases. In-depth crash databases give more information about a crash than a police report (Otte et al., 2003). A team of experts is sent on the crash scene where it is possible to take measurements and understand the causes of the crash and the kinematics of the vehicles involved in the instants before the crash. The German In-Depth investigation Accident Study (GIDAS) is the data collection project active in Germany. The measurements taken at the crash scene include among others the environmental conditions, crash information and vehicle deformation state (Otte et al., 2013). With such information the crash can be more understandable and therefore more usable in the assessment of active safety systems. A subset of GIDAS is the Pre-Crash Matrix (PCM). PCM contains the description of the pre-crash phase up to 5 seconds before the collision (Schubert et al., 2013). The pre-crash phase is the phase that precedes the collision, in which active safety systems can be applied to avoid or mitigate a collision, therefore PCM from GIDAS was chosen as one of the datasets used in this study. The PCM is divided in different files, each one containing different information:

- **Global data:** it includes the case number and the number of participants;
- **Participant data:** it includes the geometry and measures of the involved vehicles (every crash in PCM only has two vehicles);
- **Dynamics:** it includes time-varying parameters of the vehicles in the pre-crash phase, like position, speed, acceleration and yaw angle;
- **Traffic infrastructure:** it includes the description of the surroundings for road geometry, marks on the road and objects around the crash scene (trees, poles, etc.).

If in-depth studies direct the attention only to crashes, another approach in the collection of data is found in NDDs. NDDs consist in the study of everyday traffic by directly observing the driving behaviour of drivers without a particular experiment in act (Van Schagen, Sagberg, 2012). NDDs measurements can be performed by using in-vehicle recording sensors or by using a site-based approach (Van Schagen, Sagberg, 2012; Van Nes et al., 2013; Krajewski et al., 2018). Compared to in-depth crash databases, NDDs have the advantage of avoiding the trend of the underreporting of police records. In this way minor crashes and near crashes, usually not found in

police reports, can be available in NDSs, being recorded with the same importance as the more relevant crashes (Van Schagen, Sagberg, 2012). Nevertheless this approach to data acquisition brings the downside of having rare situations of near-crashes of crashes. In the USA, the National Highway Traffic Safety Administration (NHTSA) 100-Car Naturalistic Driving Study was the first study aimed at collecting data from everyday driving condition by equipping vehicles with sensors and cameras (Neale et al., 2005; Dingus et al., 2006). In the study 100 drivers were monitored for one year for a total of 43,000 hours of data, from which crashes and near-crashes were extracted. Another example of naturalistic driving study available is the SHRP2. This study included more than 3,000 people during a 3-year period. It included measurements about the vehicle state and recordings of the surroundings and of the drivers (Campbell, 2012; Victor et al., 2015).

Site-based studies can instead use cameras that record vehicle behaviour in a specific intersection or road section and they have been proven to be useful when studying the position of vehicles on the road and their relative position with the surrounding environment, including pedestrians and cyclists (Van Nes et al., 2013). A site-based NDS from the U.S. is the Next Generation Simulation (NGSIM) (Kovvali et al., 2007). It includes recordings from fixed cameras placed in strategic position aimed at recording the traffic and at computing the trajectories of the vehicles. Studies showed, however, issues in NGSIM with respect to consistency with the precision of the vehicle detection and the computation of the trajectories (Coifman, Li, 2017). This led to unavoidable problems when the dataset was used in traffic safety system assessment.

A recent site, or rather drone, based data collection was conducted in Germany. This dataset is called highD and was collected using a drone flying over German highways and recording vehicles in everyday driving conditions (Krajewski et al., 2018). The dataset quality, compared to other site-based NDDs like NGSIM, was found to be reliable and robust. In a total of 16.5 hours of recording, through image processing 110,000 vehicles with the relative time-varying parameters like position, space and acceleration were extracted. The dataset includes information about the recording time and location, the vehicles dimensions and about the time-varying parameters like position, speed and accelerations. highD is the second dataset used in this study. GIDAS PCM and highD are two of the largest and highest-quality datasets available to researchers currently, but collected from quite different perspectives and for different purposes, the former being a crash database and the latter an NDD.

The aim of this work is to, using a common simulation framework, study the possibility for highD naturalistic data to be a complement to in-depth reconstructed crash data (here the GIDAS PCM). This was done by means of what-if/counterfactual simulations, assessing AEB on both the datasets.

2 Method

In this chapter the method used throughout the work will be explained in detail. Section 2.1 describes to how the highD naturalistic driving dataset was used and how crashes were generated from it. Section 2.2 describes how GIDAS PCM was processed and how relevant metrics for the AEB implementation were extracted from it. Section 2.3 explains the AEB implementation, including a description of the framework used to simulate the AEB system to the crashes. Section 2.4 is finally dedicated to the explanation of the methods used in the analysis of the results.

2.1 highD data processing

The highD dataset for its nature of naturalistic driving dataset contains mainly normal highway cruising conditions, with a low criticality level in terms of Time to Collision (TTC) or Time Headway (THW) between vehicles. TTC is the time that a vehicle, called following vehicle (FV), has before it crashes into another vehicle, here called leading vehicle (LV), considering the initial position, velocity and acceleration of both the vehicles. THW is defined as the amount of time for a vehicle (FV) to cover a space equal to its distance from another vehicle (LV) that precedes it, keeping a constant speed.

In this dataset these manoeuvres were observed:

- *normal highway cruising*: the vehicle is driving roughly at a constant speed or slightly accelerating, without other vehicles in close proximity;
- *braking manoeuvre*: the vehicle detects a possible danger and the driver applies the brakes;
- *lane change*: the vehicle changes lane to overtake or to be overtaken by an oncoming vehicle.

In this study only the cases in which two vehicles are following each other in the same lane have been taken into consideration.

A substantial part of this work was to find critical events in the dataset and to modify the kinematics to obtain crashes, to be compared with the reconstructed crashes in GIDAS. highD, has previously been found to be more reliable and robust than other site-based NDDs, such as NGSIM (Krajewski et al., 2018), as a result of better quality recordings and more advanced image processing. In Sections 2.1.1 to 2.1.3 the process of organization of the data, assessment of critical scenarios and crash generation will be described, in turn.

2.1.1 Master clock synchronization

The first step processing highD data was to organize them from a chronological point of view. As the data were collected using a drone recording with high-quality videos, the time-varying metrics were organized based on the number of frames and the frame rate of the recording. The information from each vehicle included only the frame number of the first and last frame in which it could be found in the recording. Consequently a master clock was needed to relate vehicles one to each other and to synchronize the kinematics (e.g. the braking manoeuvres and the reaction times). A graphical representation of the process is shown in Figure 1.In particular, the process started with the time conversion of the overall recording from frame numbers to seconds. After that, the same conversion was performed with the initial and final frame of appearance for each vehicle. The expression used is the following:

$$t_i = \frac{f_i}{f_r} \tag{1}$$

where t_i is the time corresponding to the i^{th} number of frame f_i and f_r is the frame rate. After that, two equally spaced vector, with spaces of $1/f_i$, were created from the first to the last moment of appearance of both vehicles. Thus the intersection between these two vectors represented the moments in which both vehicles were in the same section of the highway and so it was the final synchronization vector. With this time vector is was the possible to cut and align all the other vectors containing the vehicle kinematics.

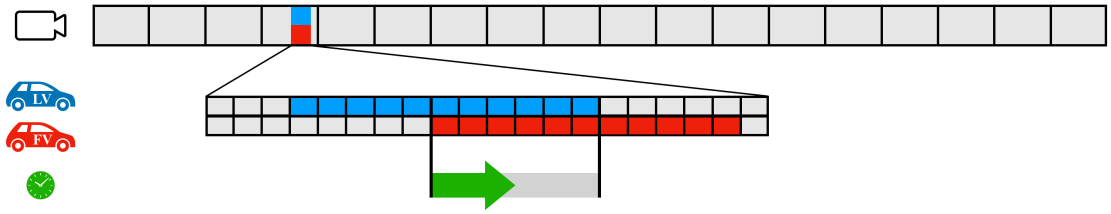

Figure 1 *Time reconstruction: from the overall recording the part containing LV and FV is extracted. The time vector is created from the first to the last moment in which both LV and FV are in the section of the highway.*

2.1.2 Assessment of critical scenarios

The second step of the highD data processing was to identify the critical events potentially useful in the generation of crashes. The criticality of the events has been defined based on parameters such as level of deceleration and THW. A scenario was defined as critical or potentially critical when the LV performed a braking manoeuvre that required a reaction from the driver of the FV.

The identification of critical scenarios started with the detection of the maximum level of deceleration of each vehicle, over the data available. Once obtained, the cases in which two vehicles were following each other were extracted. Based on this, for each of the cases involving two vehicles the THW at the instant of time in which the maximum deceleration occurred was obtained. In Figure 2 the distribution of the combination of acceleration and THW is shown for the THW less than 5 s and discarding the cases in which the LV was accelerating.

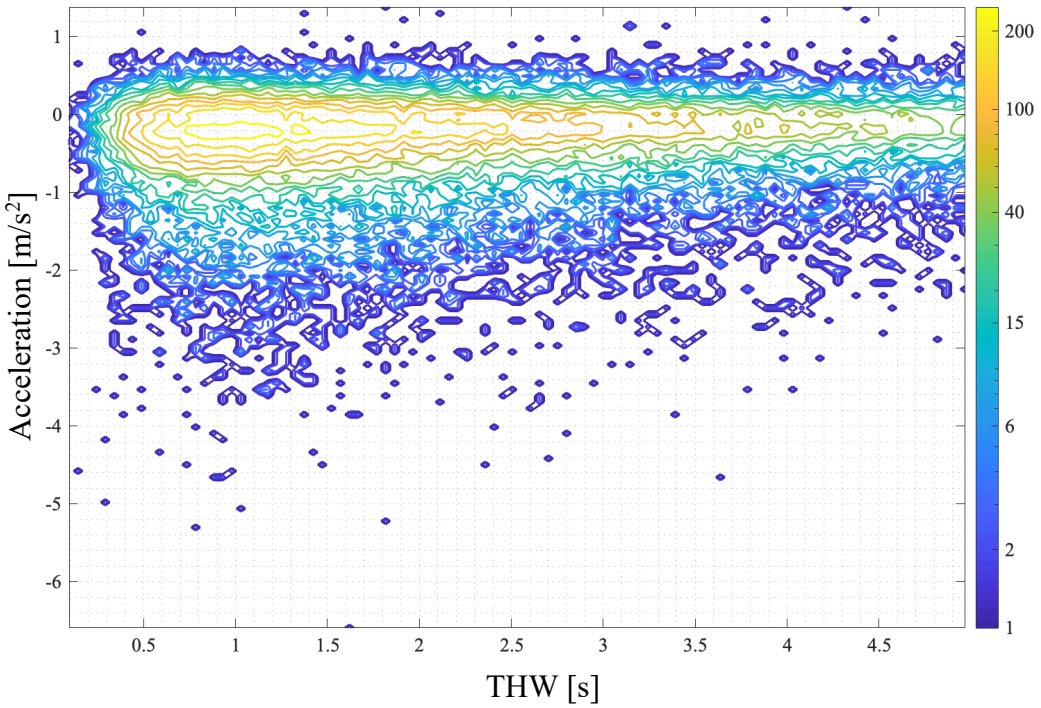

Figure 2 *Contour map of the total amount of scenarios based on the acceleration and the THW. The potential criticality of the scenario increases moving down and towards the left.*

The upper limit for the braking level was set to $-3\ m/s^2$ as it was considered a sufficiently high level of deceleration, considering also the fact that such a deceleration does not normally belong to normal highway cruising. For THW the threshold was set to 5 s, as higher values were not considered critical especially at highway speeds. With this considerations, 137 potentially critical scenarios were found, each one of them involving two vehicles and considering only the moments in which they were in the same lane following each other. In each one of the scenarios at least the LV performed a braking manoeuvre.

2.1.3 Crash generation

The crash generation process consisted in the alteration of the kinematics of the event in a way that may be reasonably argued for may be realistic, creating crashes. In all the potentially critical events the LV is performing a braking manoeuvre. The reaction of the FV, usually recorded as a similar braking manoeuvre, is what was changed in this study. The FV braking would indeed require the driver of the FV to be attentive, which is not always the case, although in this dataset the drivers were at least vigilant enough to avoid crashing – which is normally the case on our roads. A driver that is distracted or unable to react to the sudden criticality (due to sickness or drowsiness) could, however, instead have been the cause of a crash. With this argument, in this study crashes were generated by keeping the speed constant from the moment in which the braking manoeuvre of the LV was detected until the event ended up as a crash or until the end of the section of the highway (available data). To take into account fluctuations of the speed that cannot be considered a proper braking manoeuvre a threshold was set at $-1\ m/s^2$. This means that in each event the LV performed a braking manoeuvre with at least $-3\ m/s^2$, as explained in Section 2.1.2, but the FV speed was kept constant only after the LV reached a deceleration level of $-1\ m/s^2$. Lower levels of deceleration were assumed not to be caused by the brake pedal push, but for example by a simple release of the accelerator pedal. Such levels

of deceleration were not considered in this work. In Figure 3 and Figure 4 an example of the modification in the kinematics is shown, both from the point of view of positions and of speeds.

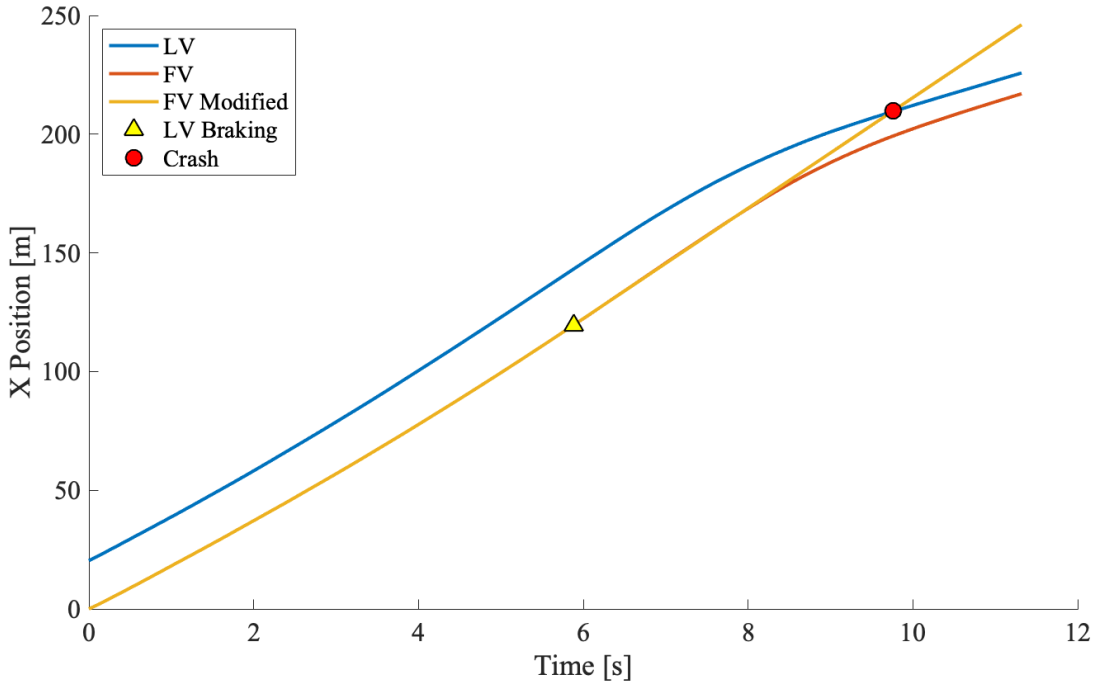

Figure 3 *Longitudinal position of LV and FV. The blue and red lines represent the original kinematics of the LV and FV. The yellow line represents the modified kinematics and the red marker is the moment in which the vehicles crash.*

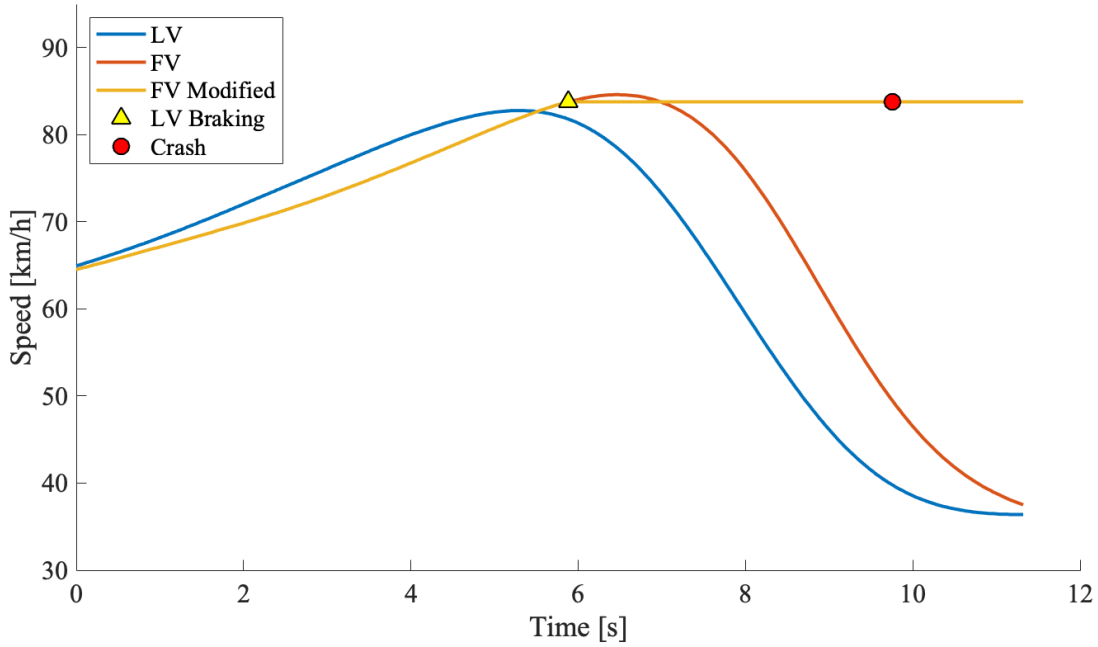

Figure 4 *LV and FV velocity in the event. The yellow line represents the constant velocity of the modified scenario that leads to a crash.*

The crashes generated from highD involved a period of time in which the driver of the FV was assumed to be distracted or unable to perform the evasive

braking or steering manoeuvre. The time elapsed from the LV braking initiation to the crash was therefore representative of the level of distraction or of inability of the driver. Figure 5 shows the relatively long times the FV driver would have to be inattentive or drowsy not to respond to the lead vehicle braking, compared to the duration of normal driving off-road glances (model from Morando et al., 2018). That is, to take into account the actual off-path glances behaviour distribution, and so to weight these results based on that, a probability density function (PDF) of off-path glances distribution could be used in relation to the raw results obtained from simulations. The process of weighting the crashes based on the off-path glance distribution was not performed in this work, as it would have required more data, and in particular more crashes with a low time from the LV braking initiation to the crash ($< 1\ s$). In addition to that, the FV driver reaction times and other aspects of the response process would have to be taking into account. This is because even if the distraction time would have been lower for each event, a reaction time of the driver would have delayed the intervention, at least some, possibly still causing the collision. The probability density function representing a lognormal normal driving glance off-road distribution was chosen based on a paper by Morando et al., 2018. Its PDF was:

$$f(x;\mu,\sigma) = \frac{1}{x\sigma\sqrt{2\pi}} exp\left(\frac{-(\log x-\mu)^2}{2\sigma^2}\right), \quad x > 0,\ \mu = -0.21,\ \sigma = 0.5. \qquad (2)$$

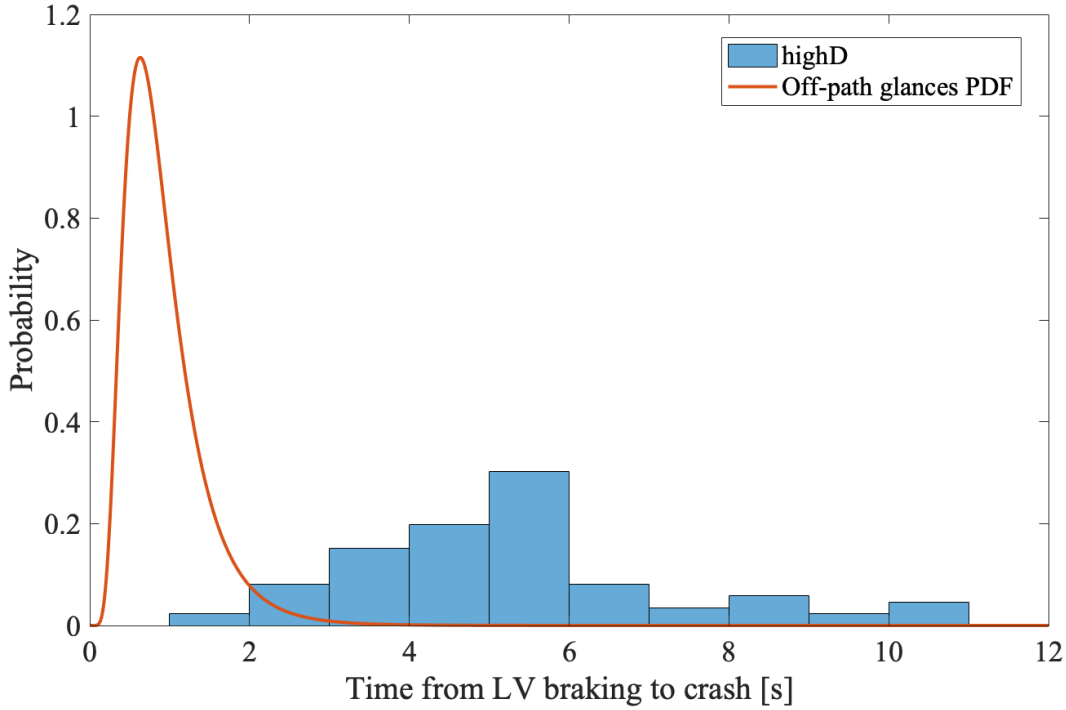

Figure 5 *Time elapsed from LV braking to FV crashing in LV. The blue distribution comes directly from the generated crashes. The yellow distribution is derived using the PDF to weight original one.*

2.2 PCM metrics extrapolation

The PCM database comes with data related to vehicles involved in the crash and to the infrastructure. The data were given in the format of ".csv" files from which, with MATLAB, the kinematics for the single vehicles and for each crash were extracted, as well as the scenario in which the crash occurred. This work focuses its attention on rear-end striking crashes on highway, so from the overall PCM database 134 crashes were selected and used. The data about position, velocity, acceleration and yaw angle

were recorded at 100 Hz. To be able to implement active safety systems like AEB or AES the PCM had to be analysed to extract data related to a possible interaction between the two vehicles. What was needed in this case was:

- **range** – defined as the distance from the FV front bumper to the closest obstacle found on the predicted future path;
- **lateral offset** – defined as the space required for the FV to move laterally both on the right and left side to avoid the crash by steering.

In Sections 2.2.1 and 2.2.2 the procedure used to obtain this data is described.

2.2.1 Range

An AEB system requires data in real time about speed, acceleration, yaw angle, yaw rate and range from the sensors available in the vehicle. The range is the only metric that is not directly available in the PCM database. It was therefore necessary to derive it from the other available metrics.

The first step of the procedure required the construction of a dynamic predicted future path for the FV. This path was based on the position, yaw angle and velocity of the FV measured in each timestep of the overall event. The yaw angle signal was first filtered with a moving average filter with a width of the window of 25 samples to reduce the noise both in the yaw angle signal and in its derivative, the yaw rate. For each timestep the current yaw rate was measured and it was used to build a trajectory that could be either straight or curved with a constant curvature. The intersection between the path and the rectangle representing the LV, if available, was then used to compute the distance between the vehicles.

The LV and the FV were approximated as two rectangles, using the metrics about length "l", width "w" and distance from the centre of gravity (COG) to the front bumper "d_{COG-fa}" of both vehicles. In PCM the x and y positions are taken at the COG, so the four vertices of the rectangles were placed having as a reference the COG, centred at $x = 0$ and $y = 0$. The vectors containing the coordinates of the vertices are the following:

$$p_A = \begin{bmatrix} d_{COG-fa} - l \\ -w/2 \\ 0 \\ 1 \end{bmatrix} \; p_B = \begin{bmatrix} d_{COG-fa} - l \\ w/2 \\ 0 \\ 1 \end{bmatrix} \; p_C = \begin{bmatrix} d_{COG-fa} \\ w/2 \\ 0 \\ 1 \end{bmatrix} \; p_D \begin{bmatrix} d_{COG-fa} - l \\ -w/2 \\ 0 \\ 1 \end{bmatrix} \quad (3)$$

and the rectangle joining them is:

$$p_{RECT} = [p_A \quad p_B \quad p_C \quad p_D] \quad (4)$$

To get the actual position in the x-y plane, first the rectangle was rotated according to the current yaw angle ψ, using the rotational matrix:

$$\widehat{Rot}(z) = \begin{bmatrix} \cos\psi & -\sin\psi & 0 & 0 \\ \sin\psi & \cos\psi & 0 & 0 \\ 0 & 0 & 1 & 0 \\ 0 & 0 & 0 & 1 \end{bmatrix} \quad (5)$$

The rotated rectangle was then given by:

$$p_{ROT} = \widehat{Rot}(z) \cdot \; p_{RECT} \quad (6)$$

Then the rectangle was translated to the current "x_{POS}" and "y_{POS}" using the translation matrix:

$$\widehat{Tras}(\vec{s}) = \begin{bmatrix} 1 & 0 & 0 & x_{POS} \\ 0 & 1 & 0 & y_{POS} \\ 0 & 0 & 1 & 0 \\ 0 & 0 & 0 & 1 \end{bmatrix} \tag{7}$$

and the final translated rectangle was given by:

$$p_{TRAS} = \widehat{Tras}(\vec{s}) \cdot \ p_{ROT}. \tag{8}$$

The process is explained in

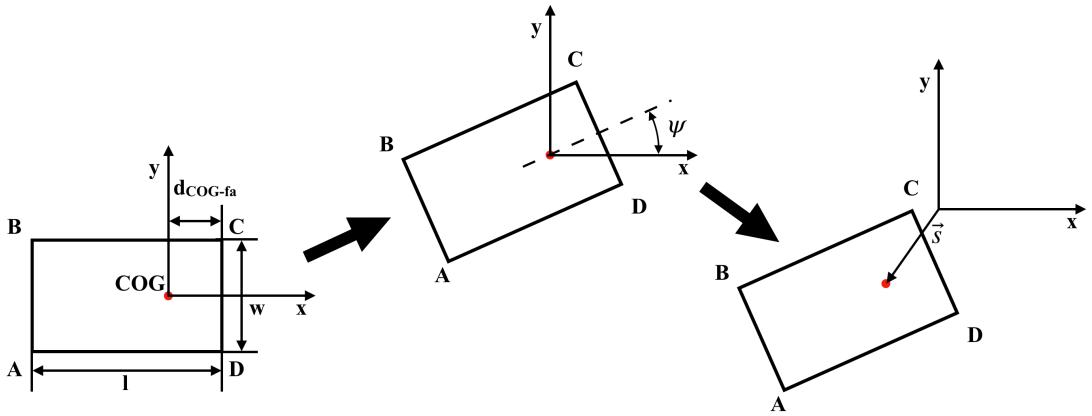

Figure 6 – The three steps process to obtain the vehicle vertices in each time step of the event. To the first configuration a rotation is applied about the z-axis, then a translation is performed along the $\vec{s}$ vector.

Once the vehicle was rotated and translated it was possible to create the predicted future path. The yaw angle ψ was derived finding the yaw rate $\dot{\psi}$ vector, for each time step. In this way by assuming constant the yaw rate in the future, a curved path (or straight, in case of $\dot{\psi} = 0$) was obtained. The radius of curvature ρ computed at the centreline of the path was obtained from the speed v_{FV} and the yaw rate $\dot{\psi}$ with the following relation:

$$\rho = \frac{v_{FV}}{\dot{\psi}}. \tag{9}$$

The predicted future path is considered as the path that the FV will follow, keeping velocity and yaw rate constant. To assess whether the scenario could have led to a crash the presence of the LV in the predicted path was considered. In Figure 7 a graphical representation of a typical scenario is represented. LV, FV and the path were designed and plotted as polygons in MATLAB.

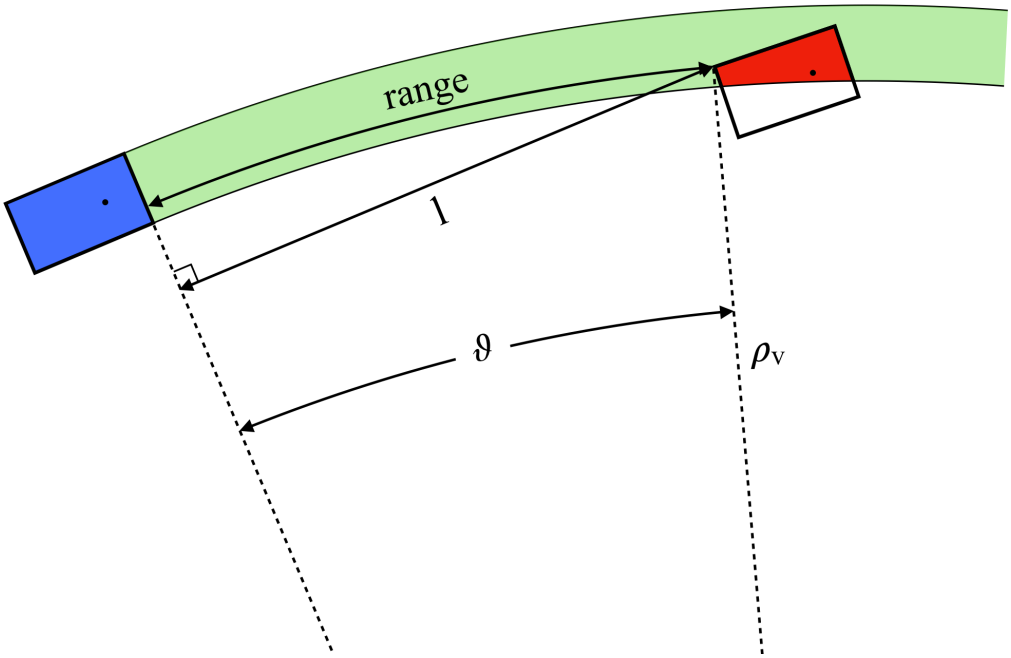

Figure 7 *Graphical representation for the procedure to obtain range from PCM. The predicted future FV path is green, the FV is blue and the LV is white. If the FV is turning, the future path follows a constant curvature. The kinematics of the LV are unchanged. The intersection area (red) defines the vertices of the LV needed to compute the range between the two vehicles.*

Once the LV, FV and predicted path were obtained, the range was extrapolated from the scenario. Two different approaches were used based on the yaw rate of the FV. If the FV was travelling with $\dot{\psi} = 0$ then the range, i.e. the relative distance between FV and LV l, was computed as a point to line distance where the points were the vertices of the LV and the line was the one passing through the vertices of the front of the FV. On the other hand, in the time steps for which $\dot{\psi} \neq 0$, the range was computed as the arc of circumference belonging to the future path, from the front bumper of the FV to the closest vertex of the LV. First the distances between the vertices of the LV and the centre of curvature ρ_v were computed. The point to line distance l was computed as for the case with $\dot{\psi} = 0$, but in this case it was used to obtain the angle ϑ and the actual relative distance along the arc of circumference of the future path with the following relations:

$$\vartheta = arcsin\left(l/\rho_v\right) \tag{10}$$

$$range = \rho_v \cdot \vartheta. \tag{11}$$

This procedure was first created to get metrics from the PCM dataset but it was also used with the highD dataset, even if in that case the events contained only highway car following scenarios, in which the vehicles were always parallel one to the other without performing any lane change. Furthermore, the same procedure was used to compute the modified range obtained following the AEB activation, as explained in Section 2.3.3.

2.2.2 Lateral offset

The collision avoidance system in this work aims at reducing or mitigating crashes with automated braking (AEB). However, in some AEB systems also comfortable steering avoidance by the driver is considered in the AEB algorithm (Brännström et al., 2010), and AES systems are being developed (Eidehall et al.,2007). To prepare for future studies and an expansion of this thesis to integrate steering avoidance (human and automated), the lateral offset between the LV and the FV was extracted for all events. Specifically, the steering avoidance calculations in AEB system considering it, and in AES systems, requires as inputs the speed at which the vehicle is travelling and the lateral distance that is needed for the FV to clear the way before reaching the LV. This distance was defined as lateral offset and was not directly available in the PCM database.

The procedure used to obtain the lateral offset started from the same predicted future path used in Section 2.2.1 to compute the range. If the LV was found on the collision path, the distance from all its vertices was computed. Based on the sides in which the vertices where found with respect to the path centreline the right and left lateral offset were computed and stored for each of the timesteps.

2.3 AEB implementation

AEB systems aim at avoiding or mitigating crashes by applying the brakes in critical scenarios when the driver is no longer able to act in time to avoid the crash. Inputs coming from the sensors of the vehicle or, in this study and as explained in Section 1, from the reconstruction of the kinematics from the highD and GIDAS datasets, are sent directly to the algorithm. This algorithm performs a threat assessment and outputs the decision about the AEB activation. To simulate the AEB system a framework capable of working with the different datasets available was developed. Having defined the needed inputs for the framework to work, the actual application of the AEB system was performed using the same procedures for both the datasets. This allowed to have comparable results in terms of crash avoidance and mitigation. The framework consists of MATLAB scripts and functions and a conceptual representation of it is shown in Figure 8.

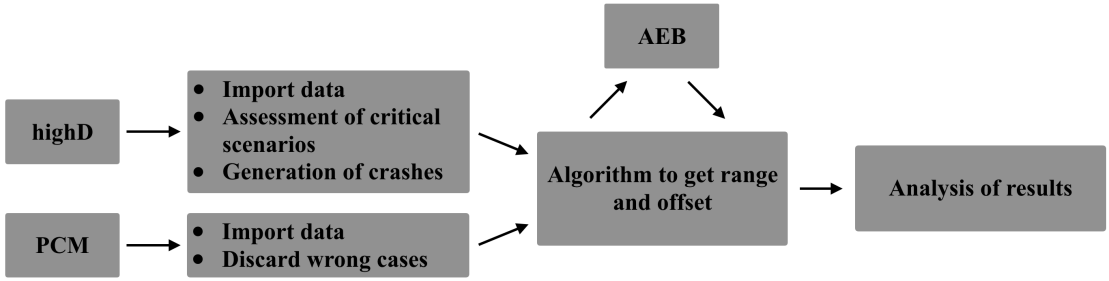

Figure 8 Framework conceptual representation.

After the collection and organization of data the process to implement the algorithm was the following:

- **Vehicle limits initialization** – Definition of the parameters about performances of the vehicle in terms of maximum deceleration achievable, maximum jerk and time delay of the braking system.
- **Algorithm selection** – Selection of different algorithms to compare the results obtained and to propose improvements.

- **Algorithm application** – Application of the chosen algorithm simulating a real time approach that reflects its implementation on a real vehicle.
- **Modified scenario** – Modification of the kinematics based on the original vehicle limits configuration, both in terms of velocities and positions of both the vehicles involved. The results of this process (see Section 2.3.3) determined whether the collisions were avoided or mitigated.
- **Result analysis** – Analysis of the outcomes in terms of number of avoided crashes and crash severity mitigation. Here results obtained from different datasets were compared and analysed.
- **Visual representation** – A visual representation of the crashes avoided or mitigated was obtained.

2.3.1 Vehicle limits

Parameters defining the vehicle limits/constraints determine the performances of an AEB system. The parameters used were the following:

- Maximum braking deceleration a_{max};
- Maximum jerk j_{max};
- Time delay of the braking system of the vehicle t_d.

The modification of this parameters affects the time and space needed for the vehicle to come to a stop when the AEB system is activated. In Table 1 the coefficient tested are reported.

Table 1 – Coefficient for AEB implementation (from Brännström et al., 2008).

a_{max}	j_{max}	t_d
$-10\ m/s^2$	$-15\ m/s^3$	$0.08\ s$

2.3.2 Algorithm

The AEB algorithm used was based on the description of an AEB system in Brännström et al. (2008). The algorithm was developed for both avoidance by braking and for avoidance by steering, both explained here. However, in this work only the part related to longitudinal braking was considered and implemented in MATLAB. The algorithm regarding the avoidance by braking is based on the comparison between the maximum acceleration that the vehicle can reach $\widetilde{a_{max}}$ and the required acceleration to avoid the collision a_{req}. The Brake Threat Number (BTN; see Brännström et al., 2008) is defined as:

$$BTN = \frac{a_{req}}{\widetilde{a_{max}}}. \tag{12}$$

In this way if $BTN \leq 1$ the collision can be avoided. The BTN is evaluated for each time step, so that the system is able to make a decision and intervene when it is necessary by applying the brakes. The collision avoidance by steering, that could be useful for future work, was based on the Steering Threat Number (STN; see Brännström et al., 2008), defined as:

$$STN = \frac{a_{req,lat}}{a_{max,lat}} \tag{13}$$

where $a_{max,lat}$ was the maximum lateral acceleration reachable by the vehicle, and $a_{req,lat}$ was defined as:

$$a_{req,lat} = \frac{2R_{lat}}{TTC^2} \tag{14}$$

with R_{lat} being the lateral distance needed to cover by the FV to avoid by steering and TTC is the Time to Collision.

The inputs for the algorithm were the following:

- **FV velocity** v_{FV};
- **LV velocity** v_{LV};
- **FV acceleration** a_{FV};
- **LV acceleration** a_{LV};
- **Range** r;
- **Time** t;
- **Vehicle parameters** (see Section 2.3.1).

In this section the STN, $\widetilde{a_{max}}$, a_{req} and therefore the BTN are derived. From the velocities and accelerations it was possible to compute directly the range rate $\dot{r}$ and the range acceleration $\ddot{r}$:

$$\dot{r} = v_{LV} - v_{FV} \tag{15}$$
$$\ddot{r} = a_{LV} - a_{FV} \tag{16}$$

From $\dot{r}$ and $\ddot{r}$ the Time To Collision (TTC), that is the amount of time available before the collision, is computed by solving the following equation:

$$0 = r + \dot{r} \cdot TTC + \ddot{r} \cdot {TTC^2}/{2}. \tag{17}$$

The minimum real root of Eq. (17) is the TTC. Once the TTC was obtained, the STN could be derived (see Eq. (14) and Eq. (13))

First the time required to stop was computed. The kinematics of the FV are the following:

$$v(t_s + t_d) = (v_{FV} + a_{FV}t_d) + a_{FV}t_s + j_{max}t_s^2/2 \tag{18}$$

where t_s is the time required to come to a stop and t_d is the time delay of the braking system. From Eq. (18), by solving $v(t_s + t_d) = 0$, t_s is found to be:

$$t_s = -\frac{a_{FV}}{j_{max}} + \sqrt{\frac{a_{FV}^2}{j_{max}^2} - 2\frac{v_{FV}+a_{FV}t_d}{j_{max}}} \tag{19}$$

and

$$\widetilde{a_{max}} = \max\left(a_{max}, a_{FV}+j_{max}t_s\right) \tag{20}$$

where a_{max} is the maximum deceleration reachable by the vehicle, $a_{FV}+j_{max}t_s$ is the achieved acceleration in the time t_s if a_{max} is not reached. To compute a_{req} the first step was to obtain the predicted range and range rate between the FV and the LV. In particular the predicted range is

$$r(\tilde{t}) = r_0 + (v_{LV} - v_{FV})\tilde{t} + (a_{LV} - a_{FV})\frac{\tilde{t}^2}{2} - j_{max}\frac{\tilde{t}^3}{6} \quad (21)$$

where

$$r_0 = r + (v_{LV} - v_{FV})t_d + (a_{LV} - a_{FV})\frac{t_d^2}{2} \quad (22)$$

and the predicted range rate is

$$\dot{r}(\tilde{t}) = \dot{r_0} + (a_{LV} - a_{FV})\tilde{t} + j_{max}\frac{\tilde{t}^2}{2} \quad (23)$$

where

$$\dot{r_0} = \dot{r} + (a_{LV} - a_{FV})t_d. \quad (24)$$

At this point the FV acceleration is

$$a_j(\tilde{t}) = a_{FV} + j_{max}\tilde{t} \quad (25)$$

and the needed constant acceleration to avoid the impact is

$$a_m(\tilde{t}) = a_{LV} - \frac{\dot{r}(\tilde{t})^2}{2r(\tilde{t})}. \quad (26)$$

By solving $a_j(\tilde{t}) = a_m(\tilde{t})$, a_{req} is:

$$a_{req} = a_{FV} + j_{max}t_x. \quad (27)$$

The resulting expression is a fourth order equation whose coefficients are the following:

- Fourth order: $j_{max}^2/2$;
- Third order: $j_{max}(a_{FV} - a_{LV})/3$;
- Second order: $-2j_{max}(v_{LV} - v_{FV}) + \dot{r_0}j_{max}$;
- First order: $2(v_{LV} - v_{FV})(a_{LV} - a_{FV}) - 2j_{max}r_0 - 2\dot{r_0}(a_{LV} - a_{FV})$;
- Zero order: $2r_0(a_{LV} - a_{FV}) - \dot{r_0}^2$.

By taking the minimum real root of the fourth order equation, the time t_x is obtained and so a_{req} is obtained as well.

The final decision made by the algorithm was to compute the BTN and so to assess whether there was still enough time for the vehicle to reach the required acceleration or not.

2.3.3 Modification of the scenario

To assess the impact of the activation of the AEB system in a vehicle for the two datasets it was necessary to use the original kinematics of the event in simulations of the braking manoeuvre of the FV. According to the parameters defined in Section 2.3.1 the new kinematics were computed using simple equations of motion. The

acceleration was modified by making it reach the pre-fixed value of a_{max} using the maximum jerk j_{max}. The following iterative procedure was applied:

$$a_i = a_{i-1} + j_{max} \cdot (t_i - t_{i-1}) \qquad a_i \leq a_{max} \tag{28}$$

where a_i is the acceleration at the i^{th} time stamp t_i. Once a_{max} was reached it was kept constant until the end of the event or until the FV came to a stop ($v_{FV} = 0$). The velocity and space were obtained by integrating the acceleration:

$$v(t) = v_0 + \int_{t_0}^{t} a(t)\, dt \tag{29}$$

$$x(t) = x_0 + \int_{t_0}^{t} v(t)\, dt \tag{30}$$

where v_0 and x_0 are respectively the initial velocity and position of the FV. Lowering the speed of the FV, avoiding or delaying the crashes, required a time extension of the event. In highD the kinematics of the LV were already available as they came from the original behaviour of the vehicle performing normal highway cruising. In PCM however the recorded events lasted only 5 s, until the original crash instant. To account for this the LV kinematics were extended keeping the value of the acceleration constant. An explanation of the process is represented in Figure 9.

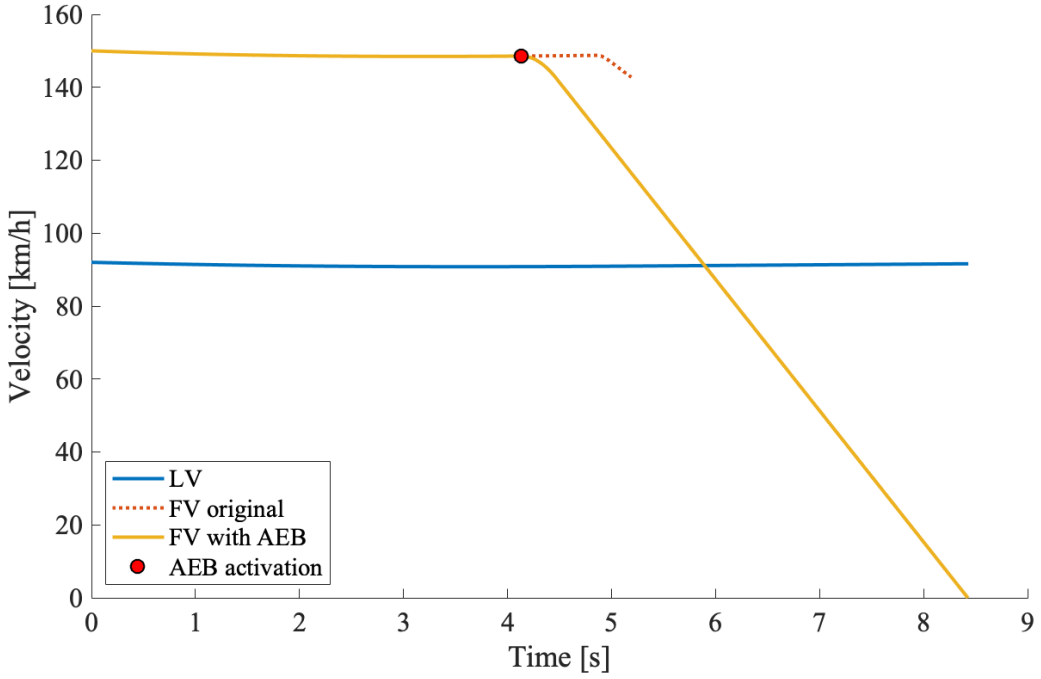

Figure 9 *The original FV velocity (red dotted line) is modified at the AEB activation (red marker) and the new braking (yellow solid line) is computed. The kinematics of the LV (blue solid line) are extended after the original 5 s available in PCM.*

Once the new kinematics for LV and FV were obtained, using the same procedure as explained in Section 2.2.1 it was possible to extract the data about the distance between the two vehicles, to assess whether the crash had been avoided or not. In this step of the process the FV was assumed to be following the predicted future path computed at the AEB activation instant, that could be curved or straight depending on the current FV yaw rate. A graphical explanation of the original and modified scenario in different time steps is shown in Figure 10.

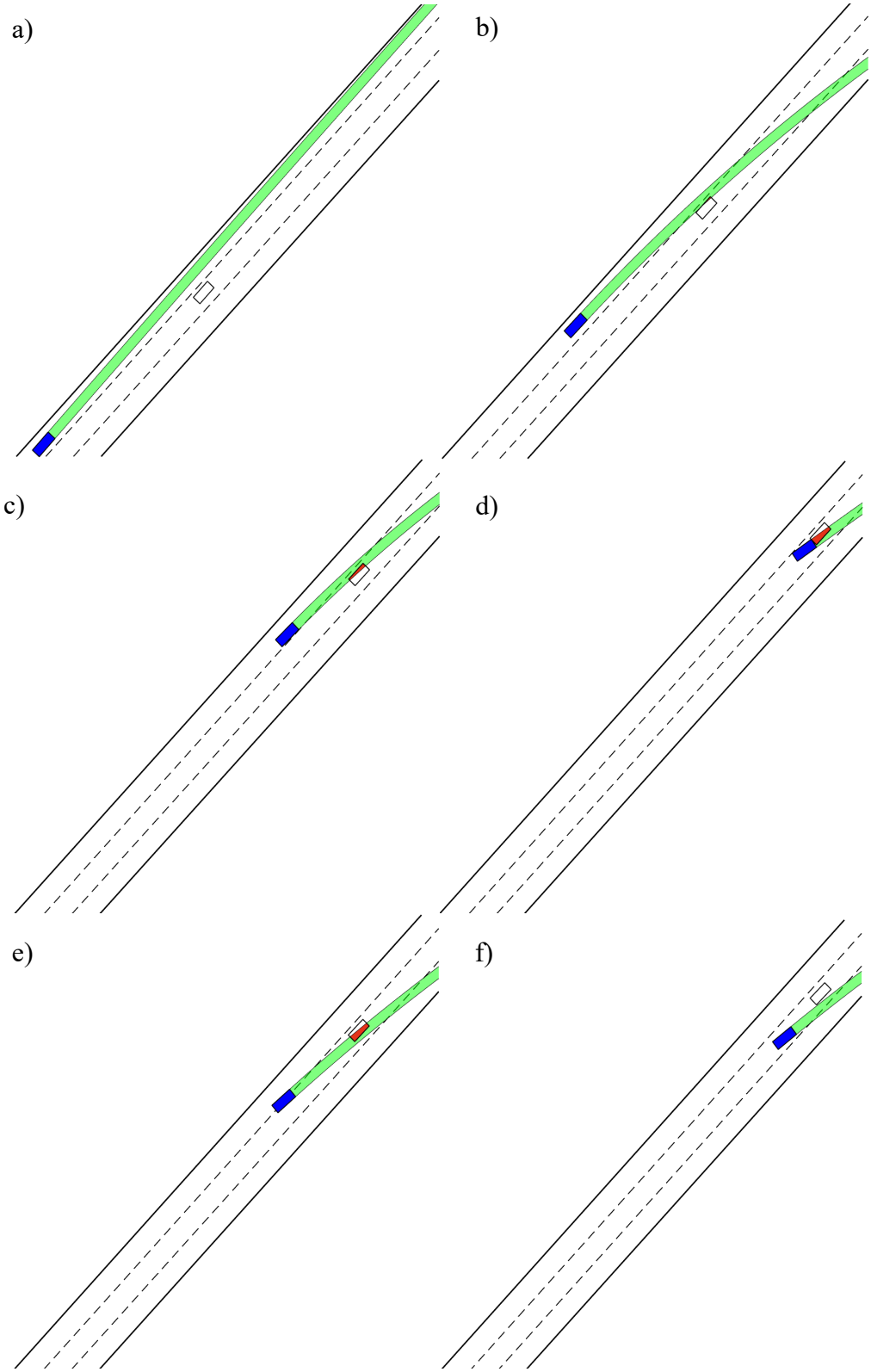

Figure 10 *Crash scenario: in a) the FV (blue) is travelling with a straight path, no collision is predicted; in b) the collision is predicted and the algorithm decides whether is the case to brake or not; in c) and d) are represented two time steps of the original crash; in e) and f) are represented two timesteps in which the AEB algorithm intervened and the crash was avoided.*

From the analysis of the new kinematics it was possible to finally assess whether the crash had been avoided or only mitigated. An example of crash avoided and crash mitigated is shown in Figure 11.

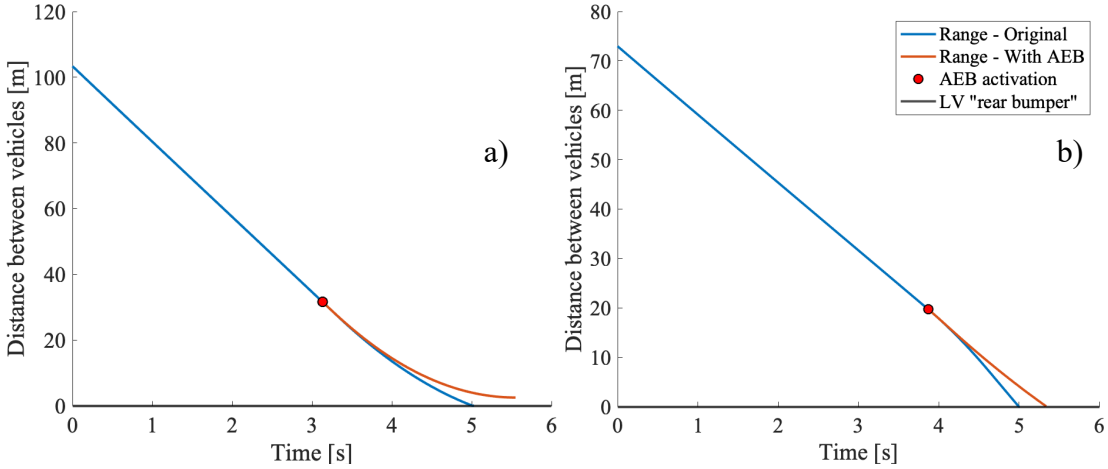

Figure 11 *Range comparison before (blue line) and after (red line) the AEB implementation. Figure a) represents an event in which the crash has been avoided, figure b) represents a mitigated crash.*

In the cases in which the crash was only mitigated the velocities of FV and LV at the new crash moment were taken and the new impact speed was computed.

2.4 Analysis methods

The results obtained in this work were divided in two different approaches. One refers to the results obtained within a single dataset, in the case of the AEB simulation. These results consisted of the analysis of the AEB performances, so in the amount of crashes avoided and mitigated. For the mitigated crashes an analysis of the difference in the impact speed was performed. The second approach consisted instead in the comparison between metrics extracted from both datasets. In particular the metrics analysed were the following:

- Impact speed before the AEB implementation;
- Range at the AEB activation;
- FV speed at the AEB activation;
- TTC at the AEB activation.

These metrics were mainly compared using histogram plots. A speed vs. TTC plot was also created to have a better understanding of the performances of the AEB algorithm in the two datasets.

3 Results

This chapter analyses the outcomes of the analysis described in Chapter 2. First a general overview on the data analysed is given, comparing the highD generated crashes to GIDAS and PCM (see Section 3.1). Subsequently, an analysis of the outcomes of the AEB application to PCM will be shown (see Section 3.2), followed by a comparison of the latter with the results obtained with the same algorithm on the highD data (see Section 3.3).

3.1 GIDAS-PCM and highD crash comparison

In this section the highD generated crashes are compared with the real crashes of the GIDAS database and with its subsection, the PCM. The comparison is based on the impact speed, defined as the relative speed between two vehicles at the crash. The crashes in highD contains only scenarios in which the LV is braking whereas the FV is not. For this reason, from the overall GIDAS highway rear-end crashes database only the crashes with these same characteristics were extracted (the LV was braking, the FV was not). The two distributions are shown in Figure 12.

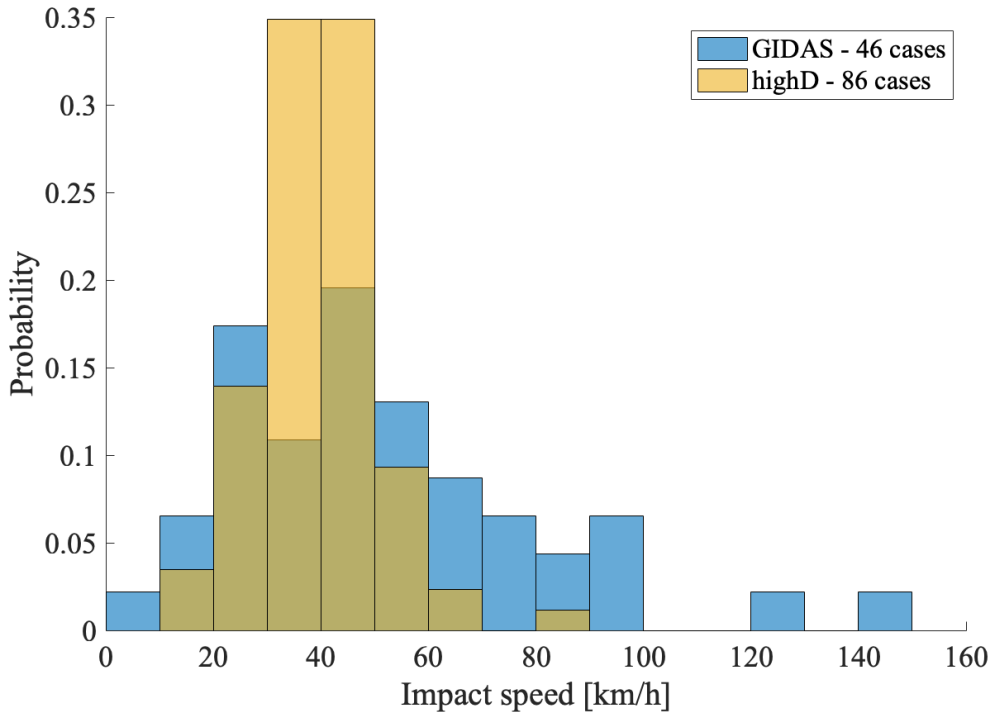

Figure 12 Distribution of impact speed. Comparison between GIDAS database (blue) and highD generated crashes (yellow).

It can be seen that the two distributions are similar, with GIDAS having some data points at high impact speeds.

As the AEB assessment was performed only on the crashes included in the PCM, a comparison between highD and PCM crashes in which the LV is braking and the FV is not is shown in Figure 13. Compared to Figure 12, for the crashes analysed in Figure 13 all the relevant metrics in the pre-crash phase are available. These crashes, together with the remaining crashes available in PCM and not included in

Figure 13 were therefore usable for further processing (see Section 3.2).

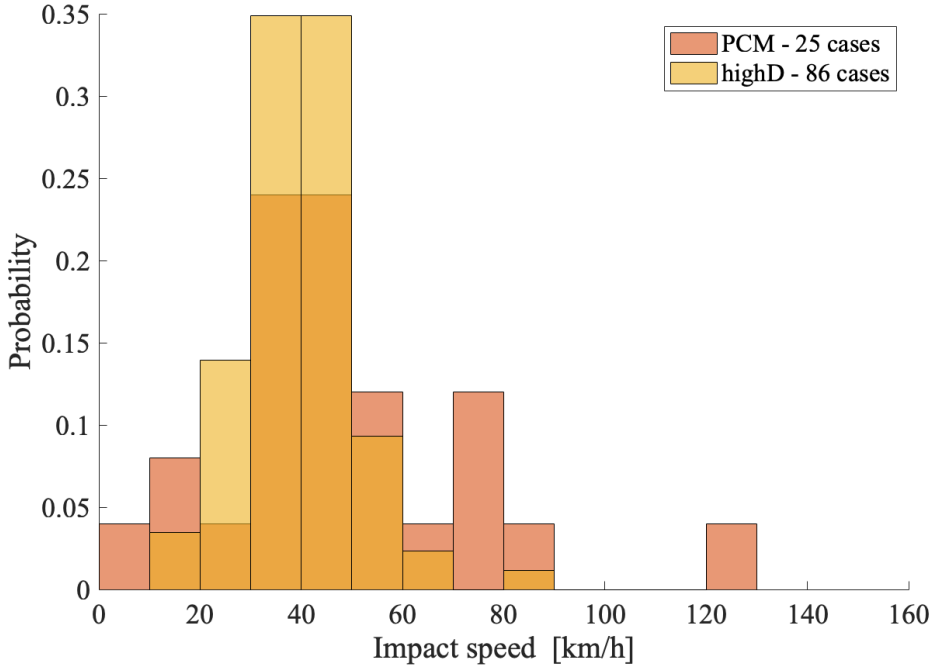

Figure 13 *Distribution of impact speed. Comparison between PCM (red) and highD generated crashes (yellow).*

Also in this case the distribution of impact speed in highD is similar to the one found in PCM, that for this scenario contains 25 crashes of the 46 contained in GIDAS.

3.2 AEB implementation on PCM

This section shows the results for the analysis of the avoided and residual crashes for AEB applied to PCM. The results obtained by the implementation of the AEB algorithm to the PCM crashes show that the collision was avoided in 112 of the 134 analysed crashes. For the 22 remaining crashes the severity of the crashes was only mitigated. In Figure 14 the distribution of impact speed of PCM crashes with and without AEB is shown.

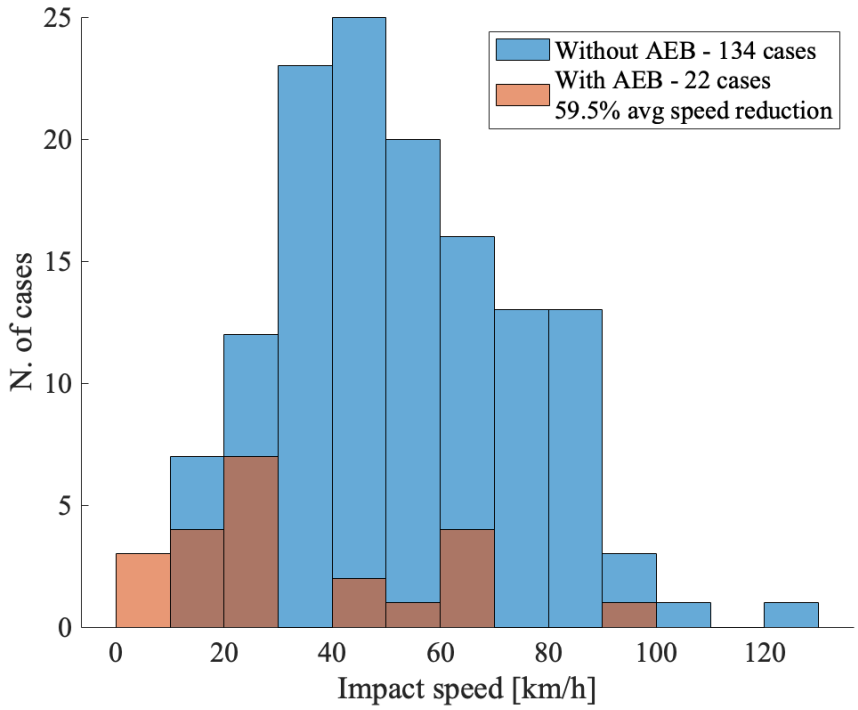

Figure 14 Distribution of impact speed: original crashes (blue) and residual crashes (red).

The average reduction in the impact speed is 59.5% for the crashes for which the severity was only mitigated. For the 22 mitigated crashes the impact speed reduction obtained in each one of the events is shown in Figure 15. In 3 of the 22 mitigated crashes the impact speed reduction was found to be less or equal to 3%. By analysing these three crashes more in detail it was found out that the low reduction of impact speed was due to unusual scenarios. In two of the three crashes there was a late lane change performed by the LV, in the last crash the FV was observed to compute an odd manoeuvre crossing all the highway and ending up crashing in an oncoming vehicle. All the three crashes share therefore a very late appearance of the LV intersecting the future path of the FV, and this led to late interventions.

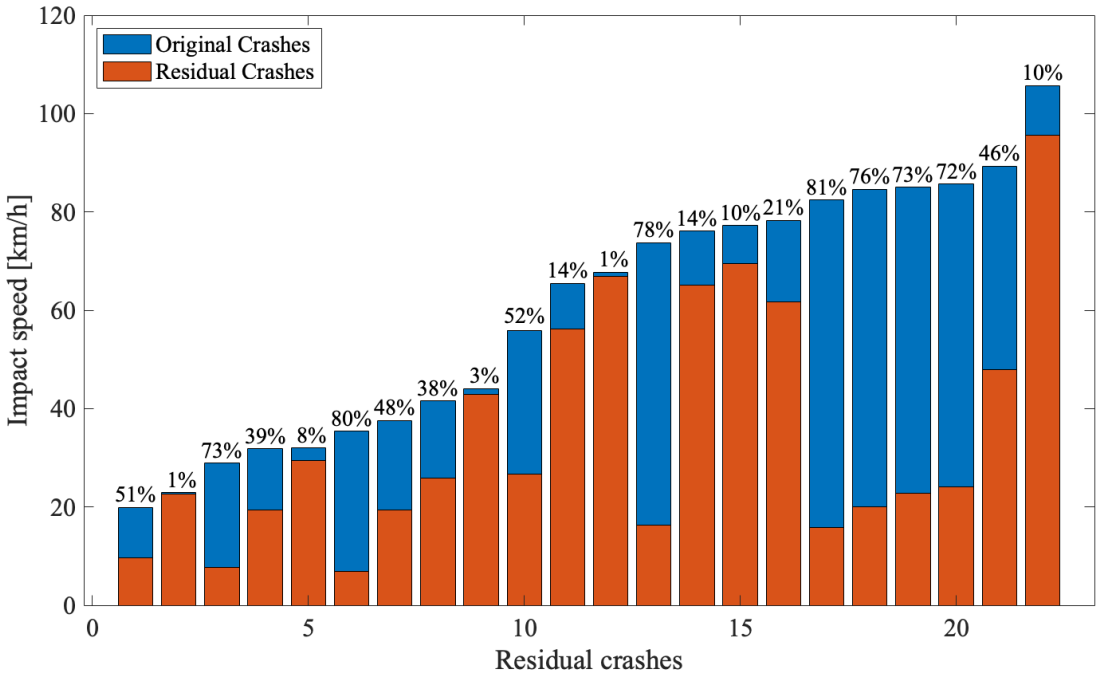

Figure 15 *Original impact speed (blue) compared with the impact speed when the AEB system is applied (red), for the 22 mitigated only crashes. The impact speed percentage reduction is shown on top of each bar.*

3.3 Comparison between AEB in PCM and highD crashes

The application of AEB on highD crashes gave as a result 100 % of crash avoidance. The results were therefore analysed from the point of view of the values of range, speed and TTC recorded at the AEB activation moment, as well as for minimum distance reached during the AEB evasive braking manoeuvre. In this section these variables are shown and comparisons are made between PCM and highD outcomes. As explained in Section 2.3.3, after the AEB application the kinematics of the FV were modified according to the specification of the braking system. The results of minimum distance between the vehicles in the cases in which the AEB avoided the crash are shown in Figure 16. The results show a majority of the cases in which the FV reached a minimum distance from the LV that was less than 4 m, both in the highD dataset and in the PCM.

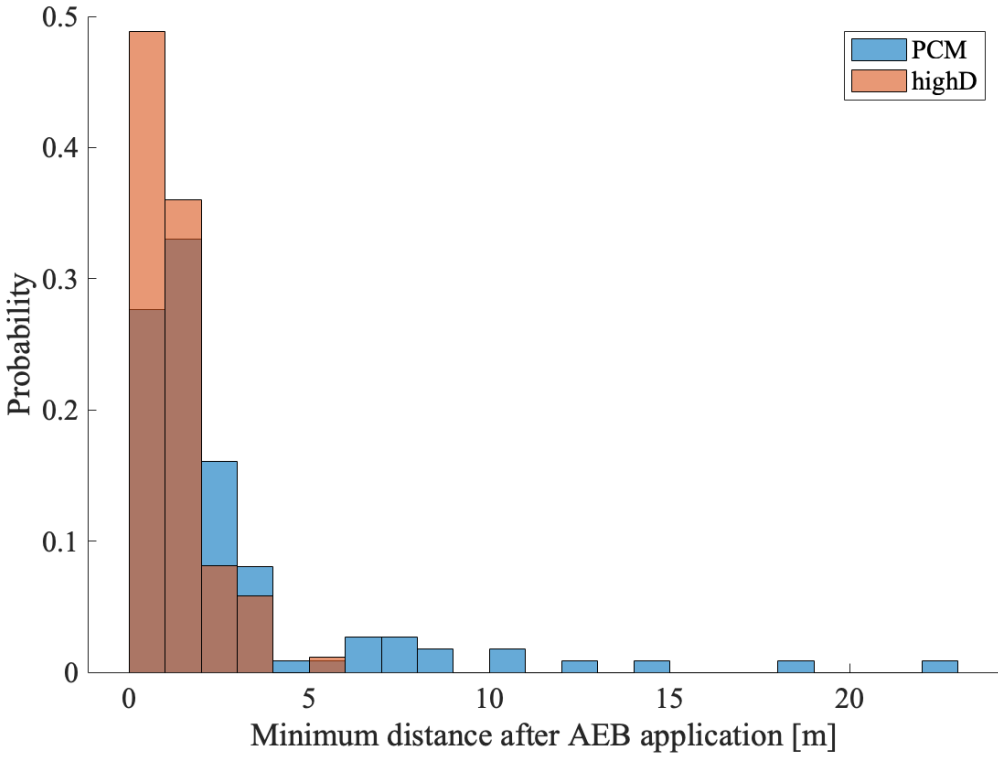

Figure 16 *Distribution of the minimum value of range (distance between the two vehicles) recorded during the AEB evasive braking manoeuvre, for the cases in which the AEB system avoided the crash, both in PCM and highD.*

The distribution showing the range at the AEB activation is shown in Figure 17. The distribution shows AEB in highD crashes was activated for relative distances less than 20 m for the majority of the cases, whereas for PCM the distribution is more spread for values under 50 m of relative distance, with outliers for which the AEB activation happened to be at 100 m of relative distance between the vehicles.

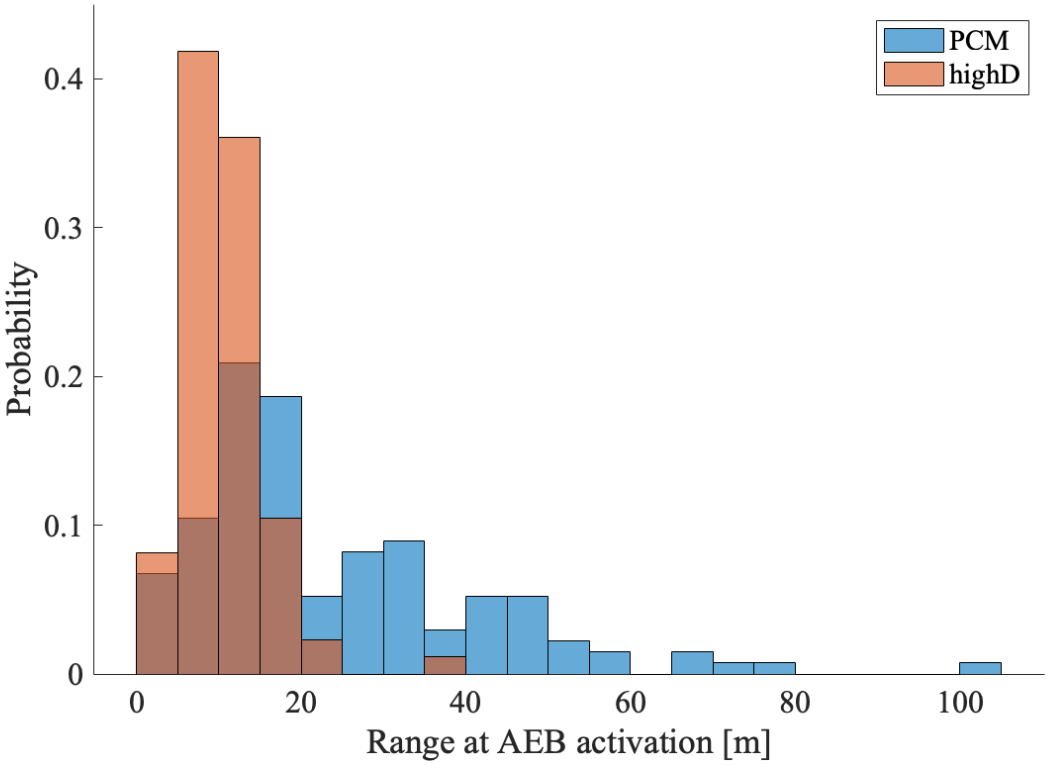

Figure 17 Range (relative distance between FV and LV) at the AEB activation.

The distribution of the speed of the FV at the AEB activation is shown in Figure 18. This comparison shows how PCM and highD crashes are more similar when referring to the speed of the FV at the AEB activation, as opposed to the relative distance plot in Figure 17.

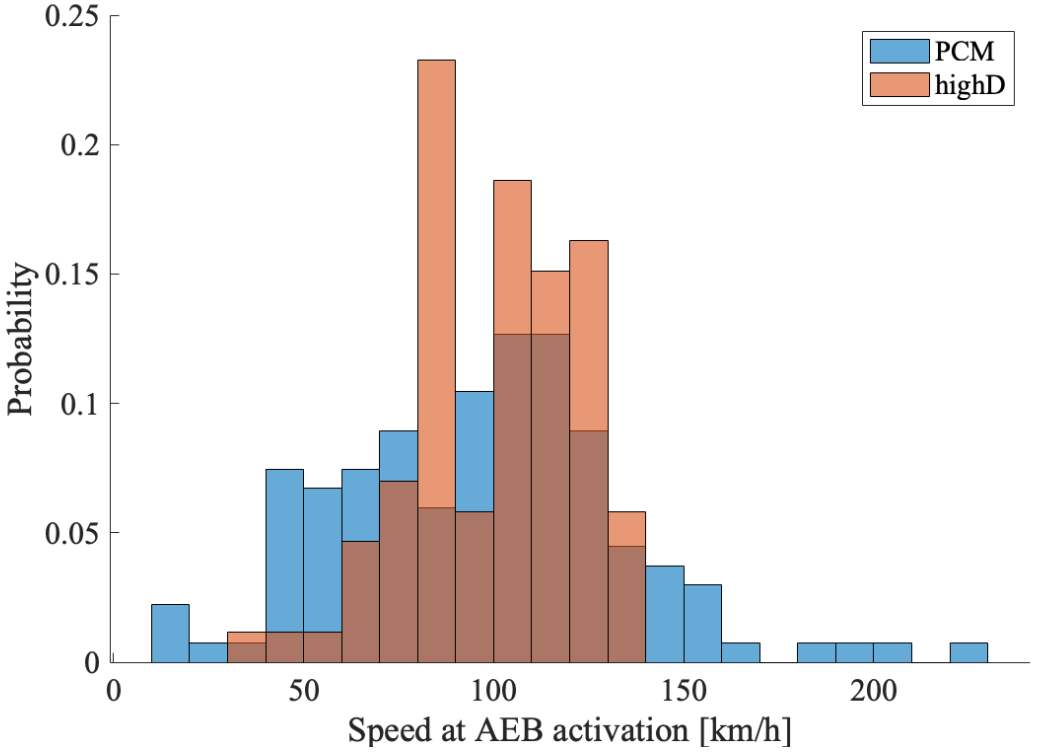

Figure 18 Speed of FV at the AEB activation.

The distribution of TTC at the AEB activation is shown in Figure 19. In this case the AEB activation happened on average at lower TTC for the highD crashes, compared to the PCM crashes.

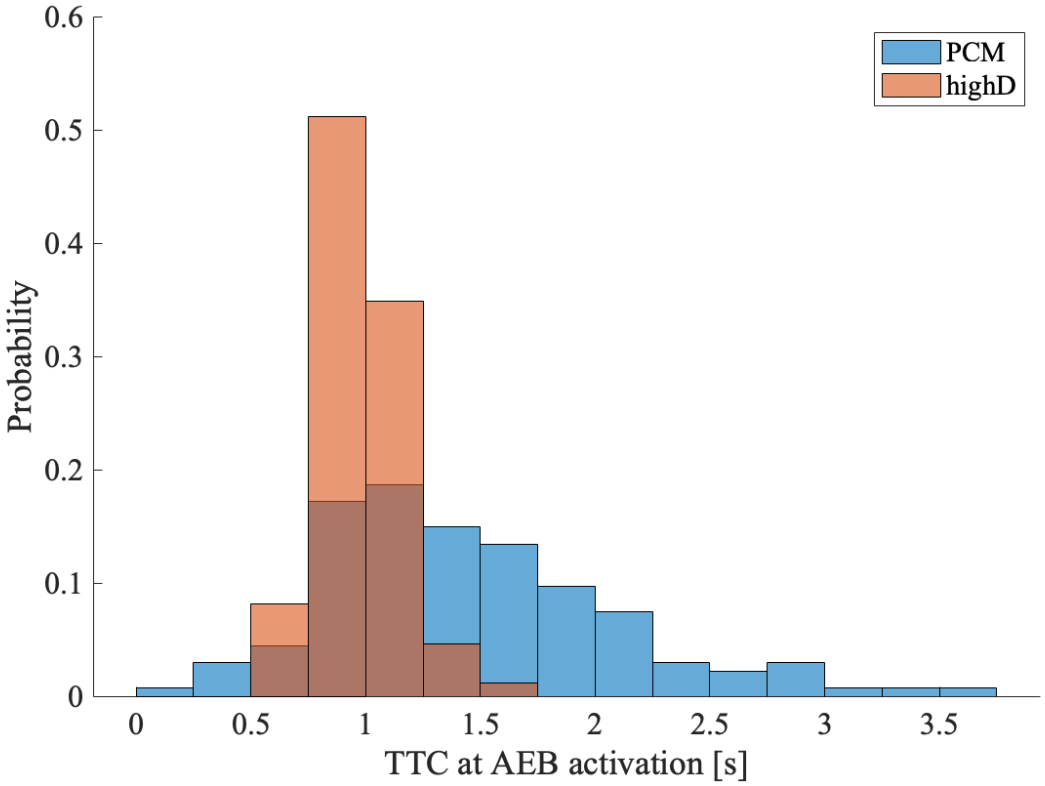

Figure 19 TTC at AEB activation.

The relation of the TTC with respect to the speed of the FV at the AEB activation for both datasets is shown in Figure 20. A linear regression model was applied to the two raw data using the "polyfit" function in MATLAB.

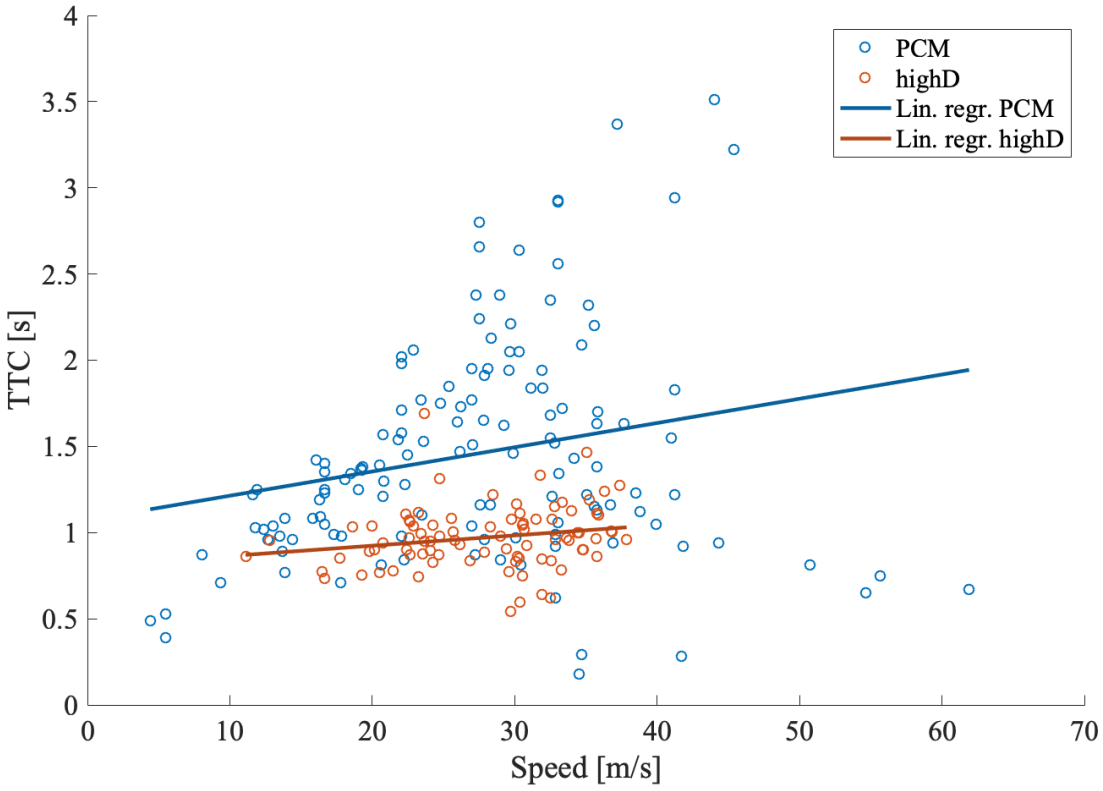

Figure 20 *TTC vs. speed of FV at the AEB activation. A linear regression model was found for both the datasets.*

The results in terms of slope were:

$$c_{highD} = 0.0060, \quad c_{PCM} = 0.0141. \tag{31}$$

and the intercepts:

$$q_{highD} = 0.8044, \quad q_{PCM} = 1.0731. \tag{32}$$

TTC and speed of the FV, plotted at the activation time, show how the majority of AEB interventions for highD crashes happens to be between TTC values of 0.5 s and 1.5 s, whereas PCM AEB interventions are found in a wider range of TTC. The result in this plot can be useful to understand the criticality of the scenario and the variety in the data analysed, as will be explained better in Section 4.1.

4 Discussion

This work aims to compare the AEB benefits and residual crashes – estimated through computer simulations – between a dataset based on crash reconstructions (PCM GIDAS; see Schubert et al., 2013) and crashes generated from naturalistic driving data (highD; see Krajewski et al., 2018). The results obtained (see Chapter 3) were first about the comparison between the original crashes available, without the AEB implemented. Then, following the implementation of the AEB on each dataset, the relevant metrics obtained from simulations were analysed between the two datasets. This section discusses the results (see Section 4.1) as well as the limitations of the study and methods applied (see Section 4.2). The section ends with an overview of the future work that could be done to improve the obtained results (see Section 4.3).

4.1 Discussion of results

The crash generation in the highD dataset followed the approach found also in other studies (Bärgman et al., 2017, Woodrooffe et al., 2013). The reaction of the FV to the braking manoeuvre of the LV was delayed and a crash was created. This led to new crashes potentially usable in the assessment of active safety systems. When generating crashes (correctly) it is possible to make them more numerous than the ones included in real crash data, while still being generated from real conditions on public roads. Note, however, that there are critics of the use of NDD for assessment and evaluation of safety, and great care needs to be taken to the validity and generalizability of the NDD-data used (Knipling, 2015).

The crashes from highD and from GIDAS/PCM were compared with respect to the impact speed. Impact speed of a crash is a metric that can be related to the risk of injuries in a crash through the computation of the delta-V (Kullgren et al., 2003). Consequently, it was considered as an appropriate variable when comparing the two sets of crashes. In particular, both the comparisons between GIDAS and highD and between PCM and highD showed similar distributions of impact speed, as can be seen in Figure 12 and Figure 13. Although the reconstructed crashes and the generated crashes were obtained in different ways, from the observation of the distribution it can be seen how the majority of cases lies in the bins at 40 km/h ± 10 km/h. This indicate that it may be possible consider generated crashes from critical events in NDS as surrogates for actual crashes, at least for subsets of crashes, as demonstrated by Bärgman et al. (2015). The severity of the crash and the possible kinematics preceding the crash (at least in terms of velocities involved) were therefore assumed to be comparable and AEB could be assessed.

The next results obtained were about the AEB application to crashes. In PCM the AEB algorithm avoided 83.6% of crashes. The 22 remaining crashes had a total average speed reduction of 59.5%. In Figure 15 each one of the mitigated crashes has been plotted in terms of impact speed before AEB implementation and impact speed after AEB implementation. As already explained in Section 3.2, the three crashes with an impact speed reduction of 3 % or lower were analysed in more detail. What was observed is that the low impact speed reduction was due to late lane changes of the LV. Such scenarios were hard to detect considering the way the framework computed the future predicted collision path (see Section 2.2), so for the algorithm to have better performances in those cases the prediction should be more advanced, based not only on the vehicles that are in front of the FV but also on its sides. Another metric used to assess the effectiveness of the AEB system was the minimum relative distance

between the vehicles reached during the FV evasive manoeuvre. The closer the FV was to the LV – still avoiding the collision – the more precise the algorithm can be considered to be. This is because when it comes to collision avoidance by braking, a major concern is in the early interventions control. Early interventions can decrease the trust of the drivers towards the systems, and they can also create safety issues. An AEB algorithm is the result of trade-offs that balance the effectiveness of the system with the aim of reducing early or false interventions as much as possible (Brännström et al., 2008). Such trade-offs, combined with the uncertainties of a real crash scenario, are the cause for which some of the crashes are only mitigated and not avoided. Therefore during the braking manoeuvre of the FV, the closer it gets to the LV the better is the algorithm at avoiding early interventions. In Figure 16 it is shown that the great majority of the minimum distances is below 4 m, for both datasets. This, considering the high speeds at which usually vehicles are driven on the highway, was found to be a reasonably good value. As can be seen in Figure 18, the AEB activates at speeds usually higher than 90 km/h, so the minimum relative distance of about 2 m is hardly improvable. The algorithm works as expected.

The same AEB algorithm was applied to both datasets. The outcomes from its application showed that all the highD crashes were avoided. This can be explained by the fact that the algorithm worked correctly in scenarios with two vehicles involved following each other, without lane changes, with easily predictable kinematics from both the FV and the LV. 22 residual crashes were found when assessing the AEB algorithm on the PCM crashes. In particular, 3 of the 22 residual crashes showed a speed reduction of only 3% or less. By analysing more specifically these crashes, they all showed a very late appearance of the LV in front of the FV, due to unusual scenarios. The outcome from PCM, containing some residual crashes, may be therefore further optimized by addressing the reasons that caused the late interventions. Nevertheless sudden lane changes, bends in the road that might limit detection of obstacles, sudden changes in the kinematics of the LV while the FV is performing the braking evasive manoeuvre are all situations that might always be difficult to be detected. The highD data outcomes suggested that to assess the complete effectiveness of an AEB system this dataset was not useful, as it did not contain critical and unexpected change in the kinematics of the vehicles that could really test the limitations of the system. A more accurate comparative analysis of pre-crash phase parameters like THW and LV decelerations could lead to a further understanding of these results, and it should be investigated in the future. Considering the process used to assess a critical scenario (see Section 2.1.2), every situation in which two vehicles were detected following each other was taken into account. This means that even the situations in which a lane change of the LV was relatively late that didn't cause the situation to be as critical as the one found in the PCM. Other datasets, also considering different scenarios rather than highway rear-end cases, could be the solution to address this problem.

The last set of results are about relative distance, speed of the FV and TTC evaluated at the AEB activation, comparing highD with PCM. The range (relative distance between FV and LV) at the AEB activation showed a distribution for highD that was narrower than the PCM one. The vast majority of cases for the highD range at AEB activation lies within 5 m and 15 m, with a maximum that is less than 40 m. This, compared to the more spread out distribution for PCM, showed how the highD crashes were much more similar one another compared to PCM crashes. The similarities within all highD crashes are, as explained before, the causes for which the algorithm had better performances on highD rather than on PCM. Similar considerations can be done for the distributions of speed of the FV, and TTC at AEB

activation. The trend for highD crashes was to have more narrow distributions, always contained from both sides from the PCM distribution. Again, the closeness of the distribution values in highD is justified by the fact that there was a low variability in these crashes.

A final comparison between highD and PCM was done through the TTC vs. speed plot. This plot allowed direct observation of the AEB system performances, by showing the TTC and the speed at the AEB activation. The trend of the linear regression showed how the TTC was directly proportional to the speed, both in highD and PCM. The overall results showed a relation between the AEB performances and the unpredictability of the crashes analysed. The AEB application to PCM, with its high variability of kinematics of the vehicles involved, lead to residual crashes that were only mitigated. The implementation on highD returned instead 100% of crash avoidance, limiting therefore the usefulness in using the generated crashes for the assessment of an AEB system. Modifications to the procedure of crash generation could lead to a more representative set of new, providing more valid estimates of the safety benefits.. However, it has to be noted that NDDs are typically used in cases of longitudinal motion only, therefore representing a substantial simplification from the actual crash scenario distribution (Bärgman et al., 2017). Further work should therefore focus on the use of NDDs for more complex crash scenarios.

4.2 Limitations

4.2.1 Methods

The process of the crash generation in highD (see Section 2.1.3) led to relatively large durations of time elapsed from the LV braking initiation to the crash moment. These results were taken into account without any modification, basically assuming the driver was asleep. A PDF function of the off-path glances duration could have been taken into account to weight differently the raw results (Morando et al., 2018). The absence of crashes in the highD generated crashes having less than 1 s of "distraction duration" (time to crash) led however to the decision to leave out this process in this study. A weighting process would have required more advanced algorithms to take into account other parameters, like the reaction times of the drivers (in addition to the need of more data at lower THWs), and this was beyond the scope of this work.

The process described in Section 2.2.1 was used to obtain the relative distance between the vehicles by computing the future predicted path of the FV and by intersecting it with the LV. This simplification was made because highway driving mainly involves vehicles following one each other in the same lane, with the same direction of travel. To improve the prediction of the future path, and so of the possible collision, an improvement could be taking into account also the current kinematics of the LV and its predicted future path. By intersecting the FV and LV future path, considering also the actual position varying in time as another variable, the crash prediction could be more accurate and realistic. In Figure 21 a graphical explanation of the intersection of future paths of both FV and LV is presented. A 3D x-y-time plot could lead to a better approximation of the vehicles future position and to a better overall crash avoidance system.

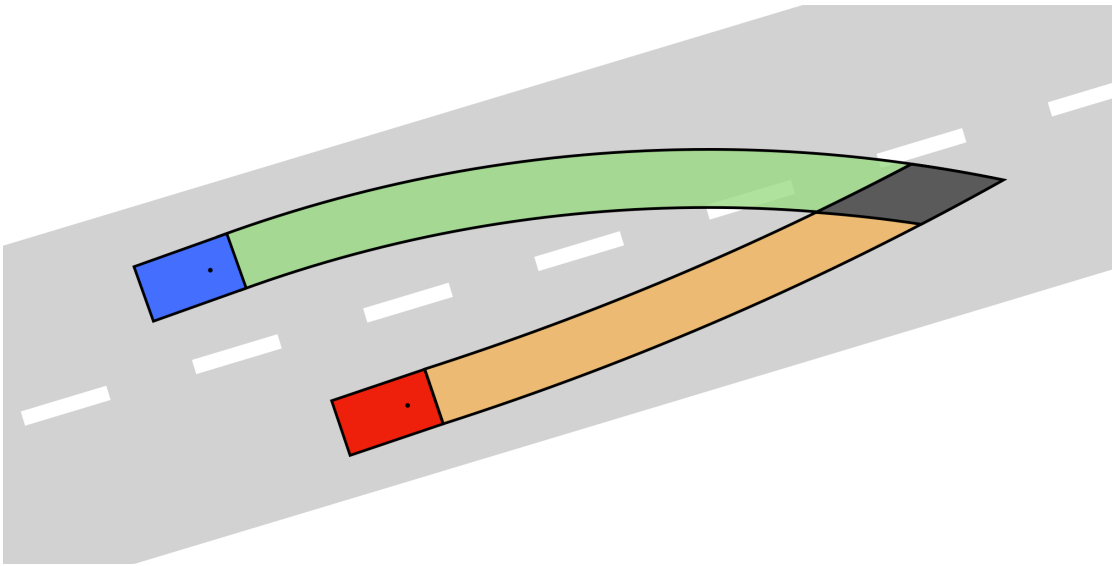

Figure 21 FV (blue) and LV (red) future paths intersection (dark grey).

The algorithm implemented in this work was taken from Brännström et al. (2008). In that paper the collision avoidance system was developed for both avoidance by steering and braking. However, due to time constraints, only braking was taken into account in this study. The limit for the jerk developed by the braking system during the AEB evasive manoeuvre set at -15 m/s^3 was taken from the same paper. This was considered a conservative approach, as in current and future vehicles this value is expected to be higher (Rosén, 2013; Jeppsson et al., 2018). Actually, to evaluate realistic and more current implementations of AEB, considerations of nuisance interventions and the consideration of drivers' abilities to comfortably avoid critical situations by steering, especially in small offset scenarios, should be included. This was, however, outside the scope of this thesis. See Yang (2019) for more information about AEB algorithms considering the driver's comfortable avoidance braking and steering manoeuvres.

The AEB application was simulated by changing the vehicle kinematics (see Section 2.3.3) after the AEB activation. The braking manoeuvre was always assumed to be as if it was on a straight path, even if the actual predicted path was curved. As before, since the crashes were only in highway scenarios the predicted path, when curved, had a high enough radius of curvature (only slightly curved). Due to that the simplification of simulating a straight path was considered reasonable. This simplification made it possible to use simpler vehicle dynamics. By using the curvature of the path and by simulating the braking manoeuvre using a vehicle model, taking the curvature into account, would have produced more realistic results. The tire would indeed need to deal with both longitudinal forces due to the braking manoeuvre and with lateral forces due to the cornering, decreasing the overall braking capabilities (Hac, Dickinson, 2006).

Another assumption relates to the modification of the scenario: the use of a maximum level of deceleration reachable during the braking manoeuvre was equal for all the modified scenarios. This means that information about the road friction coefficient were not considered. The reachable level of deceleration was selected as the assumed vehicle limit (see Section 2.3.1), which in turn determined the timing of the AEB activation. This consideration had an impact in the results of the AEB implementation as in real scenarios the reachable level of deceleration could be less than the maximum one, depending on the road condition.

In the results section (see Section 3) one of the most common metric used to compare crashes was the impact speed, that is the relative speed between FV and LV at the crash. As before, the focus of the work on rear-end crashes in highway scenarios allowed for a simplification in this aspect as well. The speeds considered when computing the impact speed were the longitudinal speeds of both the FV and the LV, as all the analysed cases were rear-end striking, and consequently they had the longitudinal speeds mostly aligned. Improvements considering the actual angle of impact could lead to more accurate results for the impact speed and crash configuration, and consequently could lead to a further development of the work, that could include studies about the injury risks derived from these crashes.

4.2.2 Data

During the analysis of the datasets some limitations in the data was identified. The general limitation related to the highD dataset is related to the amount of potentially critical scenarios (see Section 2.1.2), and the validity of the generated crashes. From the 110.000 vehicles of the datasets only 86 crashes were generated, when the crash generation procedure was applied to the most critical FV-LV interactions. The low amount of obtained crashes was mainly due to the driving conditions of most of the recordings from the highD drones. Low traffic driving conditions, in which vehicles were travelling at relative high distance one from the other, limited the amount of potentially critical scenarios. High traffic density conditions limited the collection of possible critical scenarios as well, as the low speeds involved in those situations gave as a result high levels of THW.

In addition, one other encountered problem regarded the length of the section of the highway analysed. Some critical scenarios were not usable as the generated crash would have happened after the end of the highway section. Such cases were discarded, limiting the final amount of crashes available. Some crashes had to be discarded also from the original set available in PCM. The main reason for this was that they were considered rear-end due to the collision zones of the vehicle, i.e. collisions happening between the front of the FV and the rear of the LV, but actually they happened to be side crashes, not of interest in this work.
In this study highD naturalistic driving data was used to generate crashes, given a set of assumptions. Such approaches need to be validated further. This study did show that the GIDAS PCM impact speeds when the FV was not braking (but the LV was), was similar to the generated highD crashes. For all other scenarios such assessment has not been performed.

4.3 Future work

The future work that could be done to improve and continue the current work is in part directly related to the limitations described in Section 4.2. First, the AEB assessment when using crash data and naturalistic data could have more precise results using other datasets, rather than only highD and PCM. Other AEB algorithms could also be implemented. These algorithms may use different fundamental approaches of crash avoidance (Hillenbrand et al., 2006: Hac, Dickinson 2006), and even considered nuisance interventions and comfortable avoidance manoeuvres (Yang, 2019). Avoidance by steering is one example of a potentially interesting improvement. Brännström et al., (2014) proposed a decision-making study in which the both AEB and AES could be activated depending on the kinematics of the scenario and on the driver comfort limits. The tools and inputs for algorithms

considering steering are already available from the data processing and analysis performed during this work (see Section 2.2.2).

Future work could also address some of the simplifications made during the work. The calculation of the predicted path could be improved by taking into account the future kinematics of the LV, allowing for a better estimation of time and position of a possible crash. Improvements of the modification of the scenario, considering variability in the road friction coefficient, and to the impact speed, considering the different components of the speed, could provide more realistic results. All these changes may also enable application of the algorithm to other scenarios, rather than only rear-end striking crashes on highways. For example in an intersection scenario a collision path involving the kinematics of the LV would be necessary, as the vehicles would not travel along the same direction.

5 Conclusion

In this work two crash datasets were studied and compared with respect to similarities in initial and residual crash characteristics after an automated emergency braking (AEB) system was applied to the data virtually. The first was made up of generated crashed from highway driving scenarios recorded from a drone (the highD dataset). The second was data from an in-depth reconstructed crashes dataset (GIDAS PCM). In particular the crashes were compared with respect to "original" impact speed, and by studying the effectiveness of the AEB algorithm applied to them.
The crash generation process involved the assumption of a highly distracted (or even sleeping) driver of the following vehicle (FV) that, by keeping a constant speed, crashed in a lead vehicle (LV) during its braking manoeuvre. The results showed similar results in the impact speed comparison but with relatively large differences in the estimation of the effectiveness of the AEB system. The results showed 100% of crash avoidance in the generated crashes, whereas an 83.6% of crash reduction was achieved in the in-depth crash database. The 100% effectiveness on the generated crashes shows how the LV path and behaviour was more easily predictable than in the reconstructed real crashes (GIDAS PCM). This was due to the lack of safety critical scenarios requiring late evasive manoeuvres in the highD dataset, more common in the reconstructed crashes instead. Therefore, the differences in these outcomes suggest that as of now the crashes generated from the highD dataset do not represent a viable alternative or complement to in-depth reconstructed crashes, while the initial crash characteristics (impact speed) were similar. More work in the crash generation phase, both by improving the current method and by using other sources of naturalistic driving data, is needed to further study the problem.

6 References

Abay, K.A., 2015. Investigating the nature and impact of reporting bias in road crash data. Transp. Res. Part A Policy Pract. 71, 31–45. doi:10.1016/j.tra.2014.11.002

Alvarez, S., Page, Y., Sander, U., Fahrenkrog, F., Helmer, T., Jung, O., Hermitte, T., Düering, M., Döering, S., Op den Camp, O., 2017. Prospective Effectiveness Assessment of ADAS and Active Safety Systems Via Virtual Simulation: A Review of the Current Practices, in: 25th International Technical Conference on the Enhanced Safety of Vehicles (ESV). Detroit, MI, pp. 1–14. https://www-esv.nhtsa.dot.gov/Proceedings/25/25ESV-000346.pdf

Bärgman, J., Boda, C.N., Dozza, M., 2017. Counterfactual simulations applied to SHRP2 crashes: The effect of driver behavior models on safety benefit estimations of intelligent safety systems. Accid. Anal. Prev. 102, 165–180. doi:10.1016/j.aap.2017.03.003

Bärgman, J., Lisovskaja, V., Victor, T., Flannagan, C., Dozza, M., 2015. How does glance behavior influence crash and injury risk? A "what-if" counterfactual simulation using crashes and near-crashes from SHRP2. Transp. Res. Part F Traffic Psychol. Behav. 35, 152–169. doi:10.1016/j.trf.2015.10.011

Blincoe, L., Seay, A., Zaloshnja, E., Miller, T., Romano, E., Luchter, S., Spicer, R., 2002. The economic impact of motor vehicle crashes. NHTSA Technical Report, Washington, DC. https://crashstats.nhtsa.dot.gov/Api/Public/ViewPublication/809446

Brännström, M., Coelingh, E., Sjöberg, J., 2014. Decision-making on when to brake and when to steer to avoid a collision. Int. J. Veh. Saf. J. Veh. Saf. 7 1 , 87–106. doi:10.1504/IJVS.2014.058243

Brännström, M., Coelingh, E., Sjöberg, J., 2010. Model-based threat assessment for avoiding arbitrary vehicle collisions. IEEE Trans. Intell. Transp. Syst. 11 3 , 658–669. doi:10.1109/TITS.2010.2048314

Brännström, M., Sjöberg, J., Coelingh, E., 2008. A situation and threat assessment algorithm for a rear-end collision avoidance system. IEEE Intell. Veh. Symp., 102–107. doi:10.1109/IVS.2008.4621250

Campbell, K. L., 2012. The SHRP 2 Naturalistic Driving Study: Addressing Driver Performance and Behavior in Traffic Safety. TR News, no. 282. http://onlinepubs.trb.org/onlinepubs/trnews/trnews282SHRP2nds.pdf

Coifman, B., Li, L., 2017. A critical evaluation of the Next Generation Simulation (NGSIM) vehicle trajectory dataset. Transportation Research Part B 105 362–377. doi:10.1016/j.trb.2017.09.018

Dingus, T.A., Klauer, S.G., Neale, V.L., Petersen, A., Lee, S.E., Sudweeks, J., Perez, M.A., Hankey, J., Ramsey, D., Gupta, S., Bucher, C., Doerzaph, Z.R., Jermeland, J., Knipling, R.R., 2006. The 100-Car Naturalistic Driving Study, Phase II – Results of the 100-Car Field Experiment DOT HS 810 593. National Highway Traffic Safety

Administration, USDOT, Washington, DC.
https://www.nhtsa.gov/sites/nhtsa.dot.gov/files/100carmain.pdf

Eidehall, A., Pohl, J., Gustafsson, F., Ekmark, J., 2007. Towards autonomous collision avoidance by steering. IEEE Transactions on Intelligent Transport System. 8 1, 84–94. doi:10.1109/TITS.2006.888606

ERSO, 2018a. Annual Accident Report 2018.
https://ec.europa.eu/transport/road_safety/sites/roadsafety/files/pdf/statistics/dacota/asr2018.pdf

ERSO, 2018b. Traffic Safety Basic Facts 2018: Motorways.
https://ec.europa.eu/transport/road_safety/sites/roadsafety/files/pdf/statistics/dacota/bfs2018_motorways.pdf

ERSO, 2018c. Vehicle Safety 2018.
https://ec.europa.eu/transport/road_safety/sites/roadsafety/files/pdf/ersosynthesis2018-vehiclesafety.pdf

Hac, A.B., Dickinson, J.E., 2006. Collision avoidance with active steering and braking. United States Patent US 7,016,783 B2.

Hamid, H.H., 2007. The NHTSA's Evaluation of Automobile Safety Systems: Active or Passive?, 19 Loy. Consumer L. Rev. 227.
http://lawecommons.luc.edu/lclr/vol19/iss3/2

Hillenbrand, J., Spieker, A.M., Kroschel, K., 2006. A Multilevel Collision Mitigation Approach - Its Situation Assessment, Decision Making and Performance Tradeoffs, IEEE Transactions on Intelligent Transportation Systems, Vol. 7, No. 4, pages 528-540, IEEE. doi:10.1109/TITS.2006.883115

Imprialou, M., Quddus, M., 2017. Crash data quality for road safety research: Current state and future directions. Accid. Anal. Prev. doi:10.1016/j.aap.2017.02.022

Jeppsson, H., Östling, M., Lubbe, N., 2018. Real life safety benefits of increasing brake deceleration in car-to-pedestrian accidents: Simulation of Vacuum Emergency Braking. Accid. Anal. Prev. 111 December 2017 , 311–320. doi:10.1016/j.aap.2017.12.001

Knipling, R. R., 2015. Naturalistic driving events: No harm, no foul, no validity Proceedings of the 8th International Driving Symposium on Human Factors in Driver Assessment, Training and Vehicle Design Snowbird, Salt Lake City, UT. (pp. 197-203).

Kovvali, V., Alexiadis, V., Zhang, L., 2007. Video-Based Vehicle Trajectory Data Collection. Proc. of the 86th Annual TRB Meeting. TRB.07-0528

Krajewski, R., Bock, J., Kloeker, L., Eckstein, L., 2018. The highD Dataset: A Drone Dataset of Naturalistic Vehicle Trajectories on German Highways for Validation of Highly Automated Driving Systems. IEEE 21st International Conference on

Intelligent Transportation Systems (ITSC), Maui, Hawaii, USA. doi:10.1109/itsc.2018.8569552

Kullgren, A., Krafft, M., Tingvall, C., Lie, A., 2003. Combining crash recorder and paired comparison technique: injury risk functions in frontal and rear impacts with special reference to neck injuries. In: Proceedings of The 18th International Technical Conference on the Enhanced Safety of Vehicles. No. 404, Nagoya, Japan. https://www.nhtsa.gov/sites/nhtsa.dot.gov/files/18esv-000404.pdf

Kusano, K.D., Gabler, H.C., 2012. Safety benefits of forward collision warning, brake assist, and autonomous braking systems in rear-end collisions. IEEE Trans. Intell. Transp. Syst. 13 4 , 1546–1555. doi:10.1109/TITS.2012.2191542

McLaughlin, S.B., Hankey, J.M., Dingus, T.A., 2008. A method for evaluating collision avoidance systems using naturalistic driving data. Accid. Anal. Prev. 40 1 , 8–16. doi:10.1016/j.aap.2007.03.016

Morando, A., Victor, T., Dozza, M., 2018. A Reference Model for Driver Attention in Automation: Glance Behavior Changes During Lateral and Longitudinal Assistance. IEEE Transactions on Intelligent Transportation Systems. Vol. 20, No. 8, pages 2999 – 3009. doi:10.1109/TITS.2018.2870909

Neale, V.L., Dingus, T.A., Klauer, S.G., Sudweeks, J., 2005. An overview of the 100-Car naturalistic study and findings. National Highway Traffic Safety Administration United States. https://www.nhtsa.gov/sites/nhtsa.dot.gov/files/100car_esv05summary.pdf

Otte, D., Krettek, C., Brunner, H., Zwipp, H., 2003. Scientific Approach and Methodology of a New In-Depth- Investigation Study in Germany so called GIDAS, in: The 18th International Technical Conference on the Enhanced Safety of Vehicles (ESV). Nagoya, Japan. https://pdfs.semanticscholar.org/ed7c/accc9657bea3b6a55d0a58bedbcd50a86fd9.pdf

OICA, 2015. World vehicle in use – All vehicles. http://www.oica.net/wp-content/uploads//Total_in-use-All-Vehicles.pdf

Rosén, E., 2013. Autonomous emergency braking for vulnerable road users. Proceedings of IRCOBI Conference. Gothenburg, Sweden. pp. 618–627. http://www.ircobi.org/wordpress/downloads/irc13/pdf_files/71.pdf

SAE, 2015. J3063. Active Safety Systems Terms & Definitions. https://www.sae.org/standards/content/j3063_201511/

Sander, U., 2018. Predicting Safety Benefits of Automated Emergency Braking at Intersections. Department of Mechanics and Maritime Sciences, Chalmers University of Technology. https://research.chalmers.se/publication/504728/file/504728_Fulltext.pdf

Sander, U., Lubbe, N., 2018a. Market penetration of intersection AEB: Characterizing avoided and residual straight crossing path accidents. Accid. Anal. Prev., 115, 178–188. doi:10.1016/j.aap.2018.03.025

Schubert, A., Erbsmehl, C., Hannawald, L., 2013. Standardized pre-crash scenarios in digital format on the basis of the VUFO simulation input data from GIDAS. 5th International Conference on ESAR, Expert Symposium on Accident Research, 366–372.

Van Nes, N., Christoph, M., Hoedemaeker, M., van der Horst, R.A., 2013. The value of site-based observations complementary to naturalistic driving observations: A pilot study on the right turn manoeuvre. Accid. Anal. Prev. 58, 318–329. doi:10.1016/j.aap.2013.06.026

Van Schagen, I., Sagberg, F., 2012. The potential benefits of naturalistic driving for road safety research: Theoretical and empirical considerations and challenges for the future. Procedia - Social and Behavioral Sciences, 48, 692–701. doi:10.1016/j.sbspro.2012.06.1047

Victor, T., Dozza, M., Bärgman, J., Boda, C.N., Engström, J., Flannagan, C., Lee, J.D., Markkula, G., 2015. Shrp2 - analysis of naturalistic driving study data: Safer glances, driver inattention and crash risk. doi:10.17226/22297

WHO. Global status report on road safety 2018. Geneva: World Health Organization; 2018. https://apps.who.int/iris/bitstream/handle/10665/276462/9789241565684-eng.pdf?ua=1

Woodrooffe, J., Blower, D., Bao, S., Bogard, S., Flannagan, C., Green, P.E., LeBlanc, D., 2012. Performance Characterization and Safety Effectiveness Estimates of Forward Collision Avoidance and Mitigation Systems for Medium/heavy Commercial Vehicles. The University of Michigan Transportation Research Institute for US Department of Transportation (UMTRI-2011-36).

Yang, X., 2019. Characterizing car to two-wheeler residual crashes in China: Application of AEB in virtual simulation. Master thesis at Chalmers University of Technology, Sweden